Thermal and hydraulic characteristics of a geothermally influenced trout stream : the Firehole River of Yellowstone National Park

by Dalton Earl Burkhalter

A thesis submitted in partial fulfillment of the requirements for the degree of DOCTOR OF PHILOSOPHY in Zoology
Montana State University

Abstract:
The Firehole River in Yellowstone National Park, Wyoming, is thermally enriched by the effluents of three geyser basins and numerous other geothermal features. During summer months temperatures in the lower reaches frequently exceed levels considered lethal for trout, however, self-propagating populations of brown and rainbow trout exist there year-round. Hydraulic and thermal characteristics of this stream were measured from July, 1974, to September, 1977, as part of a broader study of the thermal environment and biology of these resident trout populations. The river discharge averaged 2.1 and 7.5 m^3/s, respectively, at stations separated by 18.5 km above and below the bulk of the thermal inflow. About 1.5-2.5 m^3/s was estimated to enter the Firehole from geothermal features in the study reach, representing approximately 20-40% of total discharge during non-runoff periods.

The upper (unheated) station mean temperature ranged from 2.0 to 14.5 C, while the lower (heated) station mean ranged from 12.0 to 26.0 C. The lower station averaged about 11 C higher than the upper station. The highest temperature recorded at the lower station was 29.5 C and although this exceeds the upper lethal limit for trout, no fish kills were observed.

The power added to the river between the upper and lower stations by geothermal features was estimated as 425 MW. Average monthly solar insolation on a horizontal surface from sun and sky during critical summer months ranged from 5.2 to 7.2 kW-h/m^2-day averaging about 78% of possible clear-sky insolation. The thermal loading from solar insolation on the river surface between upper and lower stations was estimated in the annual range 26-108 MW.

Thermal infrared (IR) imagery was utilized to thermally map the river throughout the reaches where thermal inflows occur. The IR imagery identified five areas in the river where significant thermal gradients occur, some of which very probably influence fish movements.

THERMAL AND HYDRAULIC CHARACTERISTICS OF A GEOTHERMALLY INFLUENCED TROUT STREAM: THE FIREHOLE RIVER OF YELLOWSTONE NATIONAL PARK

by

DALTON EARL BURKHALTER

A thesis submitted in partial fulfillment
of the requirements for the degree

of

DOCTOR OF PHILOSOPHY

in

Zoology

Approved:

Chairman, Examining Committee

Head, Major Department

Graduate Dean

MONTANA STATE UNIVERSITY
Bozeman, Montana

November, 1979

ACKNOWLEDGEMENT

The author is indebted to many for their aid in the study. Dr. Calvin Kaya was the Principal Investigator for the project of which this study was a part. He assisted in the collection of field data and in preparation of the manuscript. Drs. John Wright and George Roemhild critically reviewed the manuscript. Messrs. Lynn Kaeding, Fred Nelson, and Dick Oswald assisted in collection of field data. Personnel at the Old Faithful Ranger Station generously allowed installation of recording equipment. Mr. Aubrey Haines, former Yellowstone Park historian, kindly provided information on historical place names in the Park.

Special thanks are due Mr. John Varley, U.S. Fish and Wildlife Service, for coordinating research activities in the Park and providing access to Library materials. Dr. Morris Skinner, Colorado State University, was helpful in arranging an overflight with thermal IR equipment. The U.S. Forest Service, Boise Fire Laboratory, performed the overflight and generously loaned equipment for data reduction. Special thanks go to Mr. Harley Leach, Electronics Research Laboratory, for his indispensable help in digitizing the IR data.

Finally, special appreciation goes to my wife and children, to my parents, and to my wife's parents. Their encouragement and support was indispensable.

The study was funded in part by a U.S. Department of Energy grant under Contract No. EY-76-S-06-2228, Task Agreement 2.

TABLE OF CONTENTS

LIST OF TABLES

LIST OF FIGURES

Figure | Page

Figure | Page

ABSTRACT

The Firehole River in Yellowstone National Park, Wyoming, is thermally enriched by the effluents of three geyser basins and numerous other geothermal features. During summer months temperatures in the lower reaches frequently exceed levels considered lethal for trout, however, self-propagating populations of brown and rainbow trout exist there year-round. Hydraulic and thermal characteristics of this stream were measured from July, 1974, to September, 1977, as part of a broader study of the thermal environment and biology of these resident trout populations.

The river discharge averaged 2.1 and 7.5 m^3/s, respectively, at stations separated by 18.5 km above and below the bulk of the thermal inflow. About 1.5-2.5 m^3/s was estimated to enter the Firehole from geothermal features in the study reach, representing approximately 20-40% of total discharge during non-runoff periods.

The upper (unheated) station mean temperature ranged from 2.0 to 14.5 C, while the lower (heated) station mean ranged from 12.0 to 26.0 C. The lower station averaged about 11 C higher than the upper station. The highest temperature recorded at the lower station was 29.5 C and although this exceeds the upper lethal limit for trout, no fish kills were observed.

The power added to the river between the upper and lower stations by geothermal features was estimated as 425 MW. Average monthly solar insolation on a horizontal surface from sun and sky during critical summer months ranged from 5.2 to 7.2 $kW\text{-}h/m^2$-day averaging about 78% of possible clear-sky insolation. The thermal loading from solar insolation on the river surface between upper and lower stations was estimated in the annual range 26-108 MW.

Thermal infrared (IR) imagery was utilized to thermally map the river throughout the reaches where thermal inflows occur. The IR imagery identified five areas in the river where significant thermal gradients occur, some of which very probably influence fish movements.

INTRODUCTION

Thermal enrichment of natural waters and its effects on resident organisms have received extensive attention in the literature (Krenkel and Parker 1969; Parker and Krenkel 1970; McKee and Wolf 1963). The U.S. Environmental Protection Agency has published recommendations for temperature regimes for some freshwater fishes (National Academy of Sciences and National Academy of Engineering 1972). Numerous articles deal with heat budgets and with modeling of thermal inflows to lakes and streams (Jackman and Yotsukura 1977; Jobson 1973; Bauer and Mackenroth 1974; Morse 1970; Brown 1969, 1972; Raphael 1962; Wright and Horrall 1967).

Sources of thermal enrichment have historically included geothermal features (relatively few locations), impoundments, municipalities, industries, and electric power generating facilities. The demand for electric power is approximately doubling every ten years in the U.S. Fossil-fueled and nuclear-fission plants will provide the major share of the increase in power production in this century. Hydroelectric power is, for all practical purposes, fixed at present capacity and alternate energy sources (solar, wind, etc.) and nuclear fusion are too far away to assume a significant share of the load (Krenz 1976).

Fossil-fueled steam electric plants have reached a practical limit of about 40% efficiency and fission plants are somewhat lower in efficiency due to materials and safety considerations (Krenz 1976;

Parker and Krenkel 1970). Nuclear power plants transfer essentially all waste heat to cooling water; fossil-fueled plants transfer about two-thirds to cooling water and the remainder occurs as stack loss (Parker and Krenkel 1970). Electric power generation through conversion of magnetohydrodynamic energy may yield efficiencies up to 80% (Rosa 1968) but this process is confined to the experimental stage at this time.

Although cooling towers are utilized in many instances in transferring waste heat to the atmosphere, many present and future installations use, and will use, once-through cooling with a natural body of water receiving the final heat load. As the population increases and demand for manufactured goods and electric power continues to rise, ever increasing demands will be placed on our natural waters for cooling. As a result, the pronounced changes in biological communities which accompany thermal enrichment will continue to be more widespread.

Heat assimilated from exogenous sources (i.e. geothermal, industrial, or power generation) manifests itself as "excess temperature" in a flowing stream. Excess temperature is defined as any increase over the natural stream temperature which would exist in the absence of any exogenous source. Excess temperature decays through dissipation of heat to the surrounding environment, primarily to the atmosphere. Conduction to the stream bottom is generally considered insignificant and is usually ignored. An exception is claimed by Brown (1969, 1972) in which conduction into the stream bed amounted to 20-25% of total energy transfer for shallow streams with a bedrock bottom.

Four mechanisms of heat exchange at a water surface are recognized. They are shortwave and longwave radiation, evaporation (or condensation) and conduction (Jackman and Yotsukura 1977). Shortwave radiation (contained in solar radiation) contributes the greatest individual component of natural heat flux. Positive values (heat flux into the water is positive) in excess of 1 kW/m^2 are common during summer months. Longwave radiation contributes a lesser amount to solar insolation. A percentage of solar insolation is reflected off the water surface. Reflected radiation expressed as a percent of total incoming radiation is known as the albedo of the surface. The albedo of water is typically about five.

Longwave radiation is essentially the only constituent of back radiation from the water surface. Back radiation is temperature dependent and can amount to a negative 300-450 W/m^2 for water in the range 0-30 C. Back radiation, H_r, follows the Stefan-Boltzmann equation,

$$H_r = \varepsilon \sigma T^4$$

where ε is emissivity (0.97 for water), σ is the Stefan-Boltzmann constant (5.67×10^{-8} W/m^2-K^4), and T is absolute temperature in K.

Evaporative heat flux is dependent on wind speed and relative humidity and can amount to negative values of 400 W/m^2 for a dry atmosphere and moderate wind speeds. Positive values can occur when conditions result in condensation on the water surface. Evaporative heat flux, H_e, is given by Jackman and Yotsukura (1977) as,

$$H_e = \lambda N \upsilon \Delta p$$

where λ is latent heat of vaporization (2,495 J/kg), N is a mass transfer coefficient (typical value, 2.42×10^{-8} kg/m-N), υ is wind speed (m/s), and Δp is the difference between the saturation vapor pressure at the temperature of the surface and the partial pressure of water vapor in the surrounding air (N/m^2).

Conductive heat flux is dependent on evaporative heat flux and the ambient air temperature. Typical values can amount to a positive or negative 200 W/m^2. Conductive heat flux, H_c, is given by Bowen (1926) as,

$$H_c = BH_e$$

where H_e is evaporative heat flux and B is the Bowen ratio,

$$B = 6.1 \times 10^{-4} P \Delta T / \Delta p$$

where ΔT is the temperature difference between air and water (positive for air temperature > water temperature), P is atmospheric pressure in N/m^2, and Δp is the difference in pressure as defined for H_e, above.

Although the decay of excess temperature is complex and nonlinear, linearized approximations exist which work well for excess temperatures within about 10 C of natural temperatures (Bauer and Mackenroth 1974; Jackman and Yotsukura 1977). Use of a model of this type allows prediction of decay of excess temperature with downstream flow. Dissipation of excess heat is a gradual process and can extend over long distances. Jackman and Yotsukura (1977) cite five of seven studies in which the remaining excess heat amounted to more than 50% of the initial excess at points 30 km downstream.

An integral part of the assessment of impacts of thermal enrichment on biological systems is the description and quantitation of thermal loading. With increasingly greater heat loads to be assimilated and more numerous sources to monitor, analysis of assimilative capacity and excess temperature becomes exceedingly complex. The biologist or engineer is faced with greater demands upon time and equipment to accomplish the task of quantifying biological impacts, temperature changes, and dissipation of excess heat to the atmosphere from the water surface. The present work was done, in part, to develop and apply some rather novel methods and techniques for describing the physical aspects of the more complex occurrences of thermal enrichment in streams. The balance of the work was done using standard procedures to describe the hydraulic parameters of a stream in conjunction with an overall assessment of the impacts of thermal enrichment on resident trout populations (Kaya 1977, 1978a; Kaeding and Kaya 1978; Kaya et al. 1977).

The stream studied was the Firehole River in Yellowstone National Park, Wyoming. This stream receives effluent from three major geyser basins of Yellowstone Park as well as numerous other geothermal features. The distribution of thermal features along the river is complex and is such that recovery can not occur from one inflow to the next. Mid-summer water temperatures in the warmest part of the river frequently exceed values considered as ultimate upper incipient lethal temperatures for trout (National Academy of Sciences and National Academy of Engineering 1972; Hokanson et al. 1977). In spite of these temperature regimes, viable trout populations exist and have been self-propagating since cessation of stocking in 1955 (Jones et al. 1978).

A comprehensive and accurate description of these complex temperature distributions and the obtaining of routine hydraulic and meteorologic data formed an important part of the overall study.

DESCRIPTION OF STUDY AREA

The Firehole River is wholly contained within Yellowstone National Park (Fig. 1). Its sources originate just under the east side of the continental divide at elevations approaching 2,560 m. From Madison Lake (el. 2,506 m) near the headwaters, it is a small cold stream flowing about 14.5 km to Kepler Cascades, which forms a natural barrier to upstream fish movement. Station A (2,317 m) was located about 0.5 km above Kepler Cascades for measurement of discharge and temperature. The stream is essentially uninfluenced by geothermal inflow above Kepler Cascades.

About 3 km below this point the Old Faithful Geyser area (2,246 m) is encountered. This is part of the Upper Geyser Basin and the first significant thermal contributions occur here. The stream flows 4 km from here to its confluence with Iron Spring Creek (2,210 m). The Little Firehole River joins Iron Spring Creek just above its junction with the main Firehole. The Little Firehole River is a small cold stream while Iron Spring Creek is warmed by numerous thermal inflows. Above the confluence of the Little Firehole River, Iron Spring Creek averages somewhat higher in temperature than the main Firehole.

From Kepler Cascades to the Old Faithful Area, the river flows through a deep narrow canyon with a gradient of about 1.5%. The substrate is a mixture of bedrock, boulders, sand, and gravel. The bedrock is rhyolite lava which occurs throughout the Firehole drainage

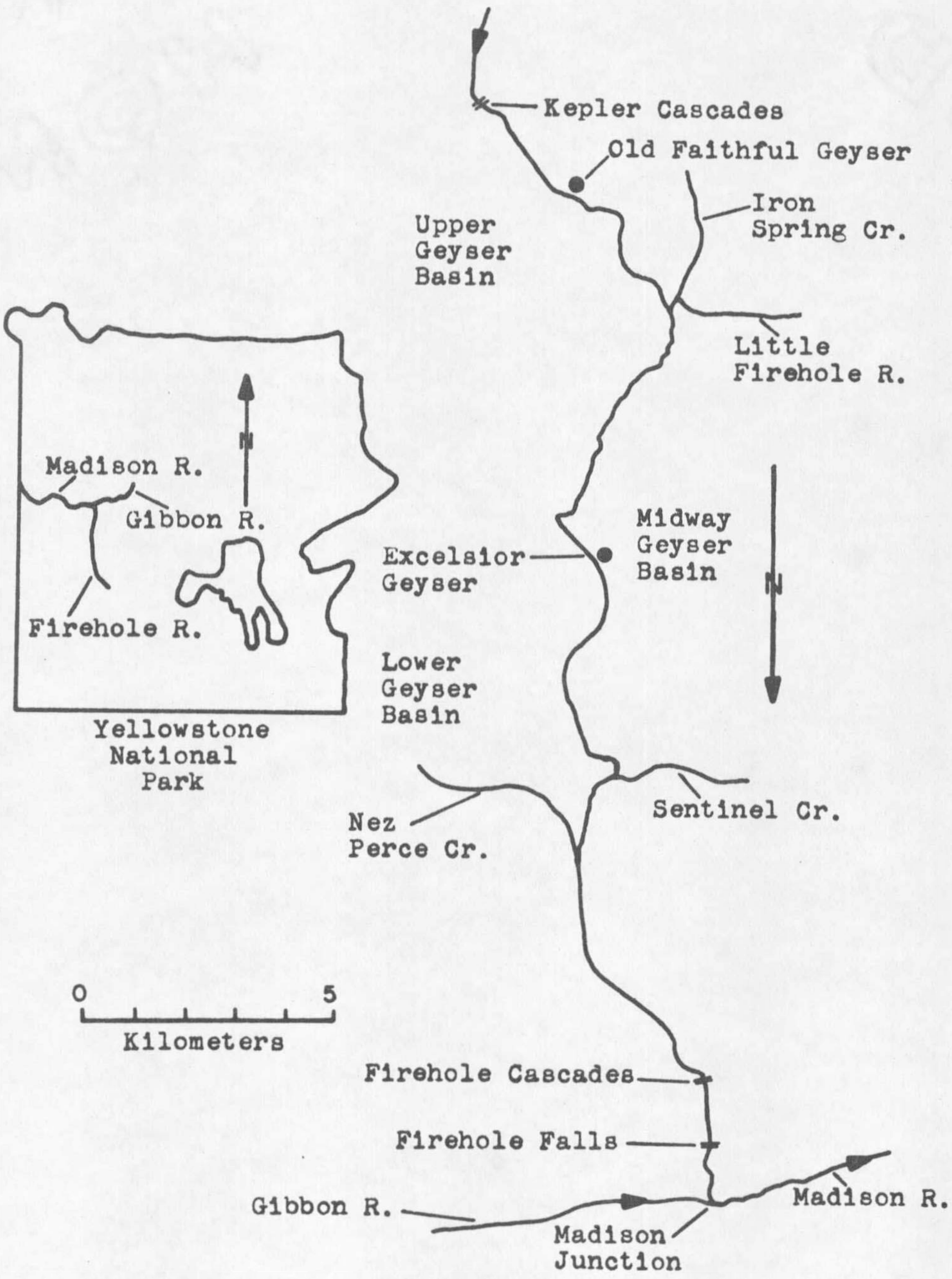

Figure 1. Map of lower 28 km of Firehole River and its location in Yellowstone National Park. Note north arrow on inset differs in direction from principal map.

basin (Alt and Hyndman 1972). From Old Faithful to Iron Spring Creek the river flows through a wide valley and is largely unshaded and shallow. The gradient is about 0.60%. The substrate is bedrock with limited areas of sand and gravel.

Below the confluence of Iron Spring Creek the river flows 7 km (gradient 0.25%) through alternate meadow and forest to Midway Geyser Basin (2,201 m) where a second concentration of geothermal features discharges into it. The most notable of these is the presently steady flow (0.17 m^3/s, Allen and Day 1935) from the dormant Excelsior Geyser. Prior to its cessation of activity in 1888 this was a giant geyser erupting to 91.5 m and causing the Firehole River to rise appreciably (Haines 1977). From Iron Spring Creek to Midway, the substrate is bedrock mixed with boulders and gravel.

From Midway the river deepens in a 4 km reach to a point about 1 km upstream from Sentinel Creek. Station B (2,189 m) was established here for measurement of discharge and temperature. The stream from Midway to Station B is largely unshaded and flows alternately over bedrock, gravel, and mud. Station B was in the Lower Geyser Basin and below the bulk of the thermal inflows.

About 1 km below Station B, Sentinel Creek (small and cold, 2,186 m) joins the Firehole. Nez Perce Creek (2,181 m) joins the Firehole 2 km below Sentinel Creek. Virtually all thermal inflows of the Firehole have occurred above this point. From Station B to Nez

Perce Creek the river is unshaded and flows over bedrock, gravel, and mud. From Midway to Nez Perce Creek the gradient is about 0.25%. From Nez Perce Creek the river flows 6.5 km (gradient 0.25%) to Firehole Falls (an upstream barrier to fish movement) and thence 1.5 km to its confluence with the Gibbon River at Madison Junction (2,073 m). The combined flows become the Madison River at this point. The Firehole flows largely through forest below Nez Perce Creek and is in a deep canyon from Firehole Cascades to Madison Junction. Below Nez Perce Creek the substrate is bedrock, large boulders, and gravel.

The reach between Stations A and B is about 18.5 km and contains an elevation difference of 128 m.

Geothermal features contribute significant amounts of Na^+, HCO_3^-, Cl^-, and SiO_2 to the river which becomes progressively richer in these substances as it flows through the succeeding geyser basins (Wright and Mills 1967; Allen and Day 1935).

Above Firehole Falls the river has populations of brown trout (*Salmo trutta*), rainbow trout (*Salmo gairdneri*), and brook trout (*Salvelinus fontinalis*) in various patterns of distribution. These are the only fish species present in this stream reach which was historically barren of fish. Trout were artificially planted in the Firehole beginning in 1889. They have been self-sustaining since the cessation of stocking in 1955.

METHODS

Water temperature was measured with a standard mercury-in-glass thermometer or a hydrographic thermometer (Whitney Corporation). Continuous temperature recordings were made with Ryon submersible 30-day thermographs. Air temperature was recorded by the National Park Service at the Old Faithful Ranger Station by a mercury-in-glass minimum-maximum thermometer. Mean daily temperature was defined as the simple average of the daily minimum and maximum. Temperatures from air and water were entered into a computer program written by the author to calculate monthly means, minima, maxima, 5-day means, etc.

Discharge was determined with a Price, type AA, current meter (the Gurley Co.). Procedures used in measurements and calculations followed those of the U.S. Bureau of Reclamation (1967). Stage-discharge relationships were established at Stations A and B to verify accuracy of the measurements. These relationships were analyzed with the aid of a polynomial regression program; r-values of 0.99 ($P<.01$) were achieved. Discharge volumes were obtained by integration of hydrographs.

Solar insolation was measured with a radiometer (Fowlkes Engineering, Bozeman, Montana) utilizing a silicon photovoltaic cell. This type of radiometer is much less expensive than the standard thermopile-type and provides accuracy to ± 5% (Selçuk and Yellot 1962). This instrument was calibrated against a Kipp and Zonen pyronometer. Total radiation (power) from sun and sky incident on a horizontal surface was recorded on strip chart (Fig. 2) by a Rustrak battery-operated continuous recorder. Power-time curves were integrated with a compensating polar planimeter. Monthly means, maxima, minima, and 5-day averages were calculated by computer.

Infrared (IR) imagery from Station A to below Nez Perce Creek was obtained by an overflight conducted by the U.S. Forest Service, Boise Fire Laboratory, Boise, Idaho. The equipment was developed for use in forest fire detection (Wilson et al. 1971) but is used to advantage to map water surface temperatures (Boettcher et al. 1976; Skinner and Ruff 1973). The IR imagery was calibrated with mercury thermometer data obtained by observers stationed along the river during the overflight (ground-truth data).

IR imagery may be used to determine stream surface temperature because of back radiation from the water surface which obeys the Stefan-Boltzmann law (see introduction). The detector and associated equipment sense the radiative power from the desired target. The signal is converted to a voltage whose magnitude is proportional to absolute temperature.

Radiative power at a given temperature does not all occur at the same frequency but instead follows a wavelength distribution curve known as Planck's law. The peak radiative power occurs at a unique wavelength for any given temperature and this wavelength is found from

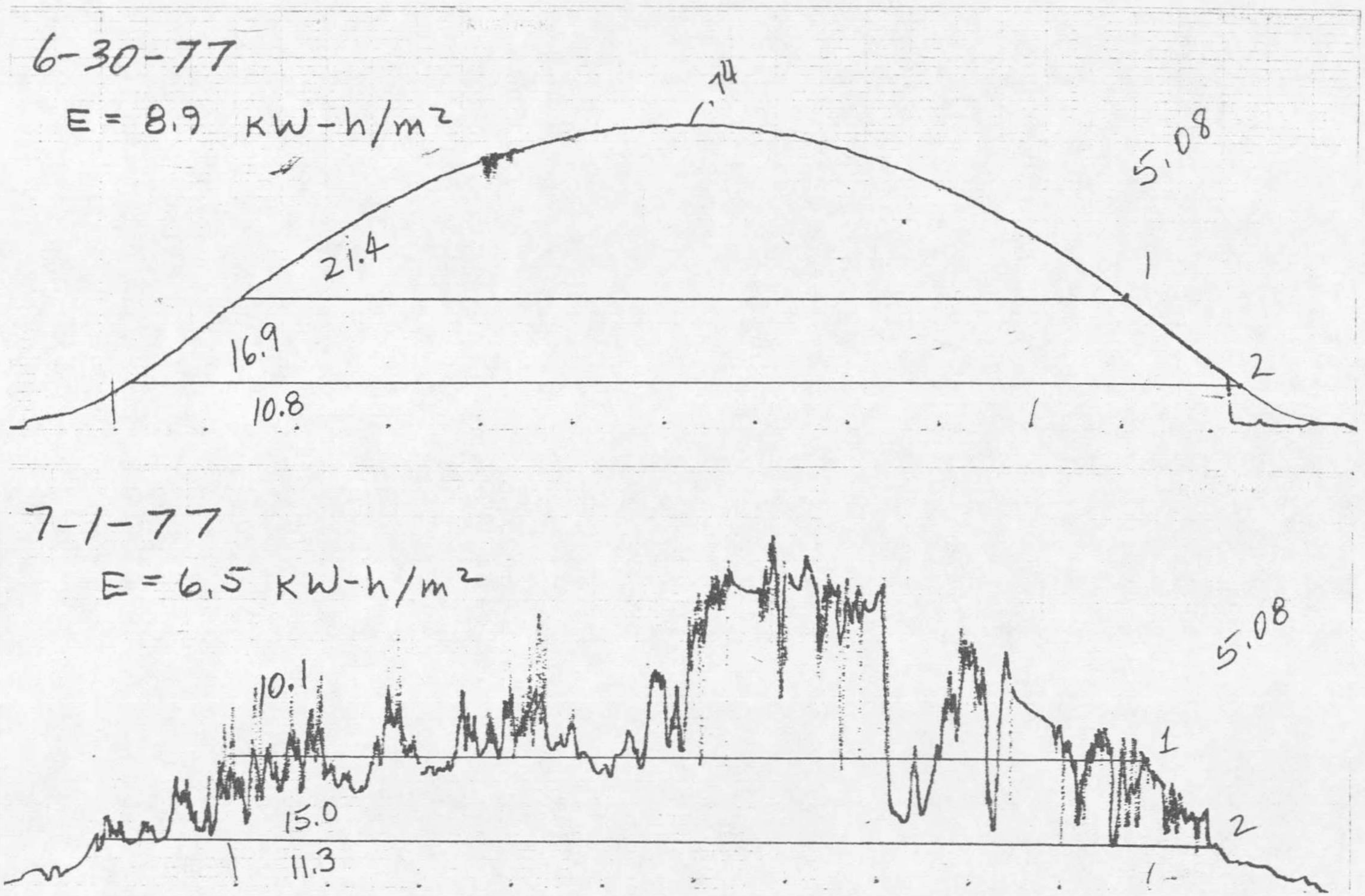

Figure 2. Typical solar insolation records for clear day (top) and partly cloudy day (bottom). Dark horizontal lines were an aid to integration of curves.

Wien's displacement law,

$$\lambda T = 2897.6 \mu m\text{-}K$$

where λ is the wavelength of peak radiative power and T is the absolute temperature. For water in the range 0-30 C the radiative power peaks in the thermal infrared region in the range 9.6-10.6 μm. These relations are described in detail by Skinner and Ruff (1973).

The IR equipment contained a scanner with a detector sensitive in the 8-11 μm range. The analog signal from the scanner was amplified and sent to a cathode-ray tube (C.R.T.) whose scan rate was synchronized with the IR scanner. The C.R.T. image was recorded on an ordinary negative-type black and white film moving past the C.R.T. The film entered a rapid processor and emerged some 20 seconds later developed and fixed providing a real-time IR image of the terrain below. The IR imagery appeared as areas of varying silver density with a direct correlation between density and temperature. At a later time photographic positives were printed from the negatives.

At the same time the scanner signal was going to the C.R.T. it was also being recorded on magnetic tape for post-flight data analysis. The analog data were digitized and stored on magnetic tape by Mr. Harley Leach of the Electronics Research Laboratory at Montana State University. Digitized data consisted of frames. Each frame consisted of selected segments of 512 scan lines (ca. 0.7 km of river reach) with each scan line equally divided into 512 parts. Each of these digitized parts was designated a picture element or "pixel" and represented the average radiation from approximately 2.3 m^2 (a square, 1.5 m on a side).

Each frame consisted, then, of 512^2 pixels. Each pixel required eight bits (1 byte) for storage. Storage requirements for each frame were then 262,144 bytes or about 2.1 million bits. Each frame was played individually through a digital-to-analog converter and into an oscilloscope. The oscilloscope image was recorded by Polaroid film allowing a visual check on the accuracy and limits of each digitized frame (Fig. 3).

The photographs of the real-time C.R.T. image and the Polaroid prints of the digitized frames provided only graphic representation of the data. A quantitation of the digital data was necessary to realize the full benefits of the IR imagery process.

Computer programs, written by the author, were used in conjunction with others written by Mr. Harley Leach to read the digitized data from magnetic tape and to assign temperature values using the ground-truth data obtained at the time of the overflight. The temperatures were output as imagery on a standard line printer by an overprinting technique (Fig. 4). Symbols used in the overprinting were taken from Macleod (1970). This imagery allowed the river to be accurately delimited.

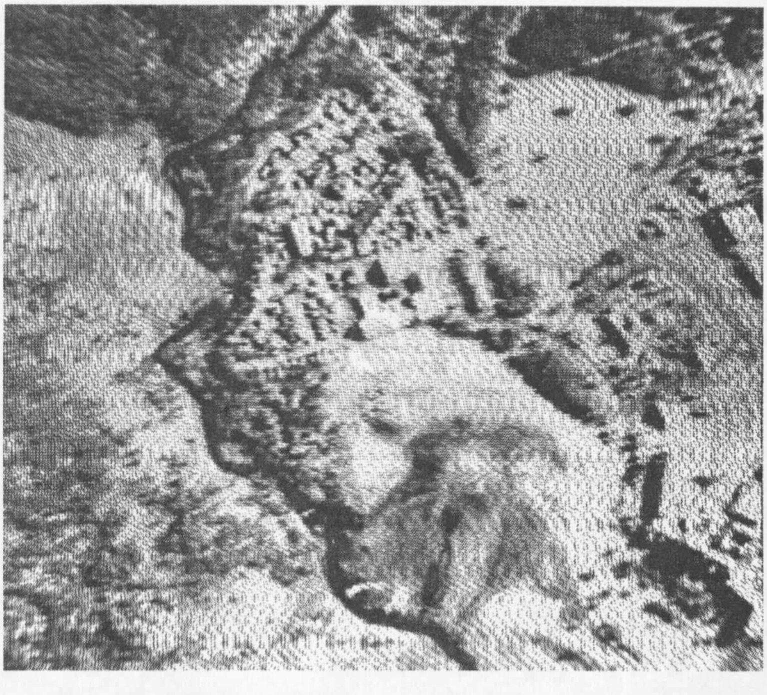

Figure 3. Typical photograph of IR imagery obtained from the C.R.T. The display illustrates a digital-to-analog conversion of data stored on magnetic tape. Pictured is Old Faithful Area.

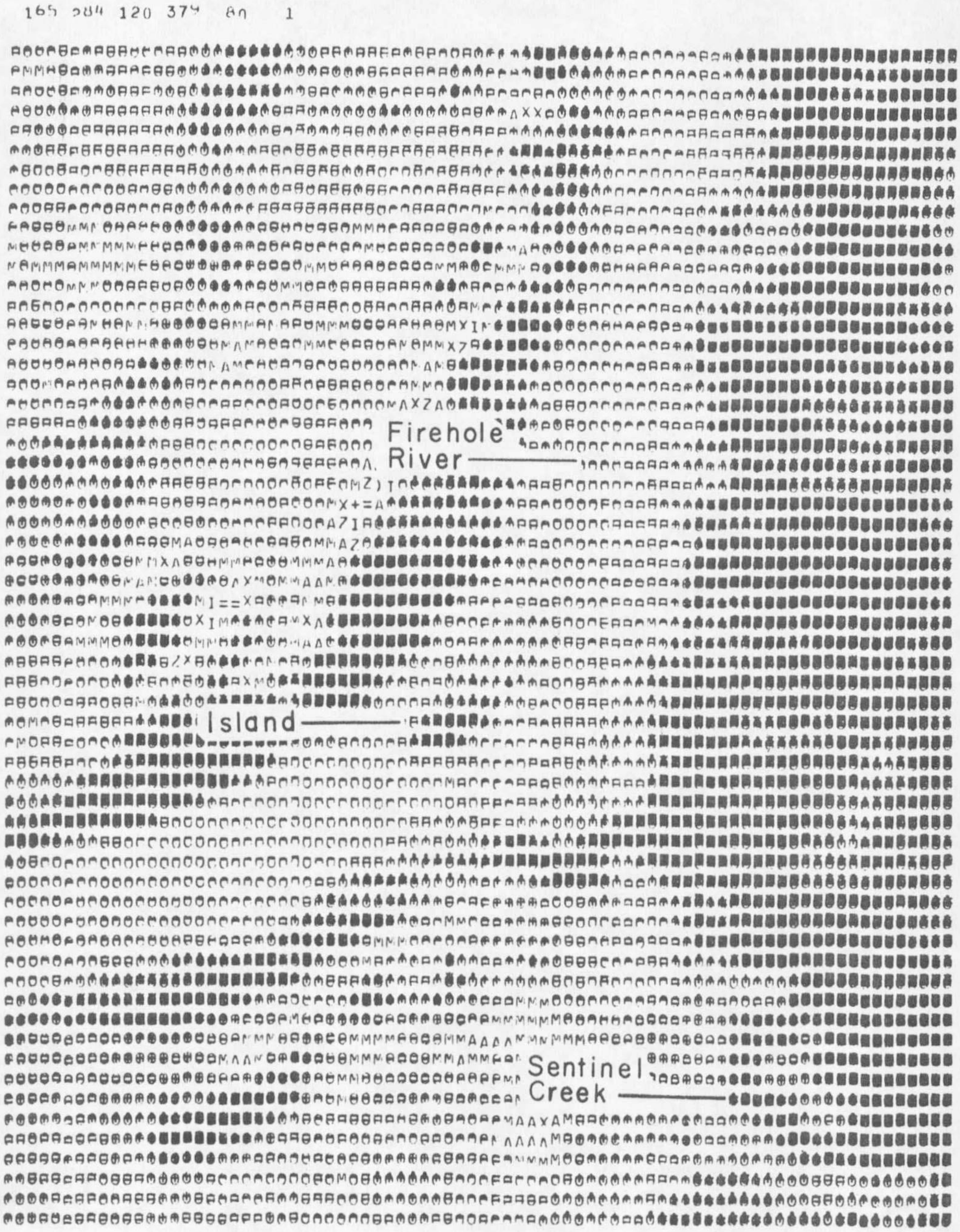

Figure 4. Typical line printer output utilizing shading to display IR imagery. Density is inversely correlated with temperature. Area featured is confluence of Sentinel Creek.

A second part of the output (also from a standard line printer) consisted of the same imagery represented by a field of digits (one digit per pixel) overprinted so that a temperature range of 0-29 C could be coded (Fig. 5). With the two parts of the printout at hand, the water surface temperature of the delimited river reach could be obtained quickly and accurately (accuracy ca. ±1 C). Furthermore, temperature gradients from thermal or cold-water inflows could be easily observed for the extent of their persistence.

Isotherms were constructed by connecting points of equal temperature along temperature interfaces. Tracings of river and isotherms made from several adjacent printouts assembled together provided graphic and quantitative presentations of temperature distributions and gradients.

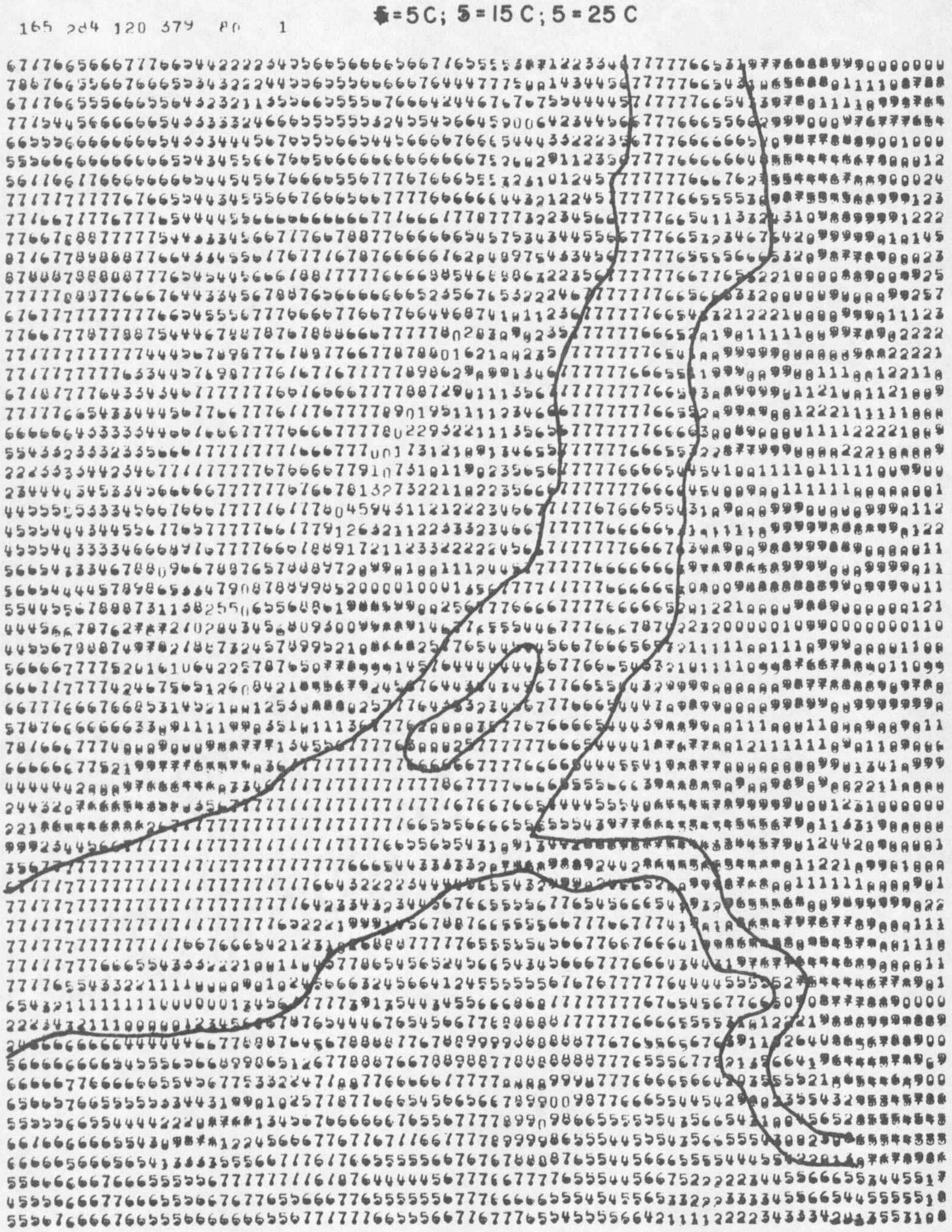

Figure 5. Typical line printer output utilizing a field of digits to display IR imagery. River was delimited by hand. Area featured is same as in Figure 4.

RESULTS

Discharge

Hydrographs for Stations A and B are shown in Figure 6 for September, 1975, through September, 1977. It may readily be observed that discharge in 1976 was significantly higher than in 1977. For the comparable periods of May-September, the 1976:1977 discharge volume ratios were: Station A, 2.8; Station B, 1.8. The lesser difference at Station B was likely due to a fairly constant and significant volume of thermal water entering the Firehole above Station B. Station A more accurately reflected surface runoff which was low due to unusually light snowpack in the winter of 1976-1977 followed by a drought in 1977 (Jones et al. 1978).

A comparison with the Madison River provides a perspective of the Firehole runoff for these two years. Annual discharge volumes of the Madison River (measured 13 km below Hebgen Reservoir and adjusted for storage in the reservoir) have been determined for many years by the U.S. Geological Survey. A comparison of discharge volumes for the years 1974-1977 with the long-term average volume (Table 1) shows 1976 38% above average and 1977 12.6% below average, a volume ratio of 1.58 (1976:1977). This ratio is lower than that for either Station A or B but it must be considered that this ratio is from a much greater watershed and full, instead of partial, water years. The value is close enough, however, to suggest that the discharge volume of the Madison is indicative of the Firehole for 1976 and 1977. Based on this comparison

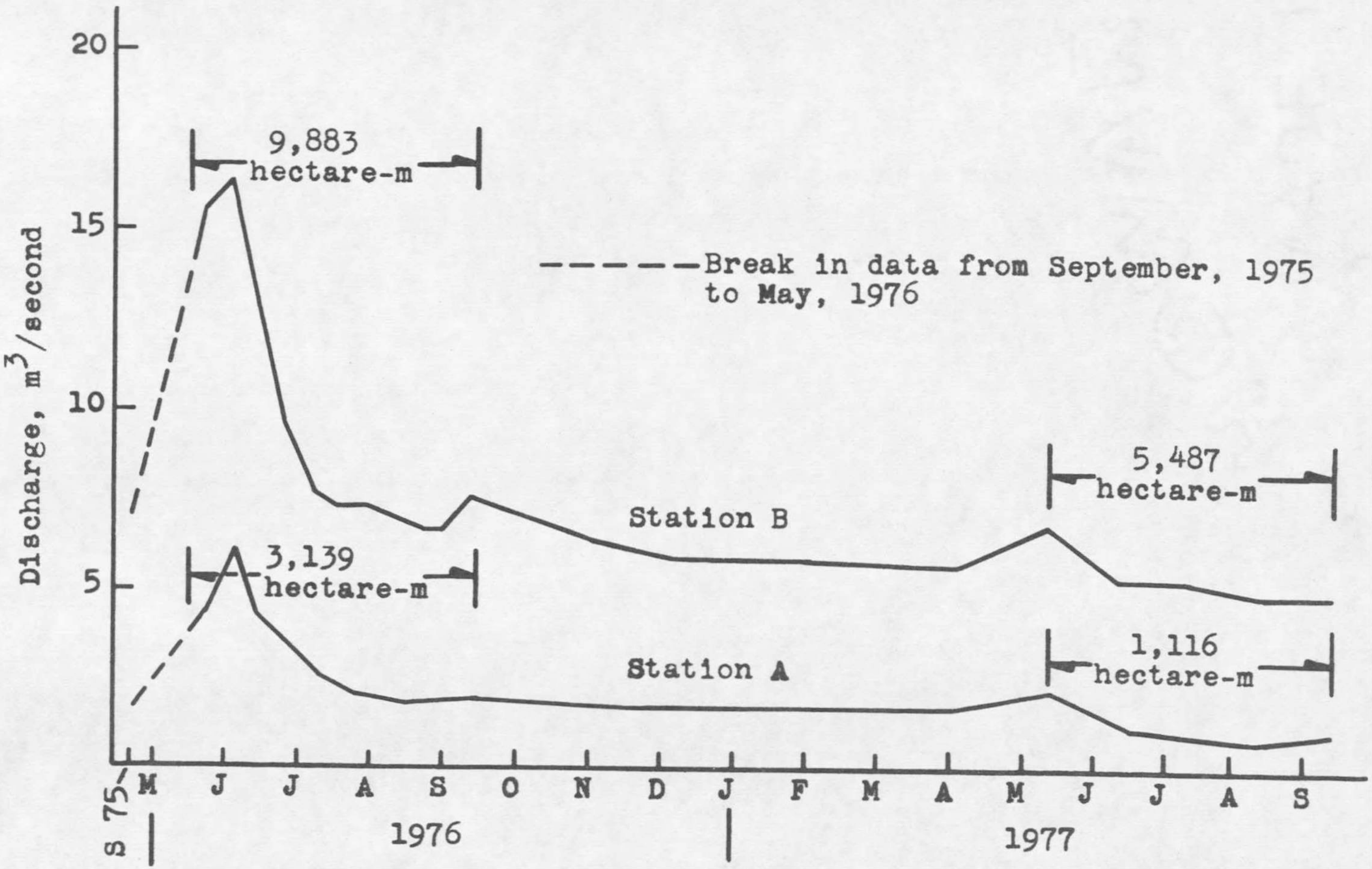

Figure 6. Hydrographs for Stations A and B. Discharge volumes for comparable time periods are shown.

the discharge volume of the Firehole was below normal for 1977, a conclusion supported by visual observations and by Jones et al. (1978).

Table 1. Annual discharge of Madison River 13 km below Hebgen Reservoir (Adjusted for storage in the reservoir) (U.S.G.S. 1974-1977).

Water Year[1]	Discharge (ha-m)	Avg. Discharge (ha-m)	% Deviation from avg.
1974	113,937	88,564 (65)[2]	+28.6
1975	110,545	88,811 (66)	+24.5
1976	123,237	89,279 (67)	+38.0
1977	77,894	89,094 (68)	-12.6

[1] Water year is defined as October of previous year through September of noted year.

[2] Number in () indicates years of record upon which average is based.

Discharge data for Stations A and B and for other locations, when available, are given in Table 2. The mean discharge at Station A for the period September, 1975, through September, 1977, was 2.1 ± 0.8 m^3/s (P=.05, N=19). The difference in average non-runoff discharge (discharge during periods of low flow when surface runoff was minimal) between Station A and a point just above Iron Spring Creek was 0.4 ± 0.7 m^3/s (P=.05, N=7). Most of this difference was probably due to thermal inflow from the Upper Geyser Basin although gains or losses to the groundwater may have influenced the value. Allen and Day

Table 2. Discharge at various locations along the Firehole River and its tributaries (m^3/s).

Date	Station A	Firehole at Iron Spring Cr.	Little Firehole R.	Iron Spring Cr. above Little Firehole R.	Sum of preceding three columns	Firehole below Biscuit Basin	Firehole at Fountain Freight Brdg.	Firehole below Midway	Station B	Sentinel Cr.	Nez Perce Cr.
9-3-75	1.7	2.2	0.8	2.1	5.1	5.5	4.8	7.1	6.9	0.3	2.0
5-22-76	4.4	...	...	...	...	...	...	...	15.5	...	...
6-5-76	6.1	...	...	...	...	...	...	...	16.4	...	...
6-25-76	3.5	...	...	...	...	...	...	...	9.6	...	...
7-6-76	2.7	...	...	...	...	...	...	...	7.7	...	...
7-18-76	2.3	...	...	...	...	...	...	...	7.3	...	...
8-1-76	2.0	...	...	...	...	...	...	...	7.3	...	...
8-13-76	1.9	...	...	...	...	...	...	...	6.9	...	...
8-28-76	1.8	2.2	0.9	2.3	5.4	5.3	5.3	6.5	6.6	0.3	...
9-11-76	1.9	...	...	...	...	...	...	...	7.5	...	...
10-5-76	1.7	...	0.9	1.9	...	...	...	...	6.9	...	...
10-30-76	1.7	...	...	...	...	...	...	...	6.4	...	...
12-4-76	...	...	...	...	...	...	...	...	5.9	...	...
1-29-77	1.6	...	...	...	...	...	...	...	5.9	...	...
4-5-77	1.6	1.6	0.6	2.0	4.2	...	...	...	5.6	...	...
5-13-77	2.1	2.4	0.9	1.6	4.9	...	...	...	6.6	...	...
6-16-77	1.2	1.6	0.7	1.6	3.9	...	...	...	5.2	...	...
7-12-77	0.8	1.3	0.5	1.6	3.4	...	...	...	5.2	...	...
8-11-77	0.8	1.3	0.6	1.6	3.5	...	...	...	4.9	...	...
9-15-77	1.0	...	...	...	...	...	...	...	4.9	...	...

(1935), who estimated thermal inflow by summing discharge from each feature, gave 0.25 m^3/s as the thermal inflow for this same reach. After its confluence with the Little Firehole River, Iron Spring Creek had a non-runoff average of 2.5 ± 0.6 m^3/s (P=.05, N=7) while the main Firehole just above the mouth of Iron Spring Creek averaged 1.8 ± 0.8 m^3/s (P=.05, N=7). Iron Spring Creek probably contributes more discharge than the main Firehole throughout the year except possibly during peak runoff periods. A large percentage of Iron Spring Creek originates from thermal features which tend to sustain its discharge throughout non-runoff months.

After joining with Iron Spring Creek the Firehole appeared to maintain a steady flow (when uninfluenced by snowmelt) until it reached Midway Geyser Basin. At Midway the river gained 1-2 m^3/s of discharge. Allen and Day (1935) gave 0.37 m^3/s as the thermal contribution from Midway. A significant quantity of thermal inflow at Midway is indicated by a temperature differential of 2-3 C between points above and below. Underwater thermal springs (Argyle 1966) may contribute inflow undetected by Allen and Day.

From Midway to Station B the late-summer discharge remained essentially constant although many thermal features enter within this reach. Allen and Day (1935) estimated an inflow of about 0.5 m^3/s of thermal water in this reach although it was not detected by discharge differential in the present study. It is quite possible that losses to the groundwater account for the apparent discrepancy. The mean discharge at Station B (for all measurements) was 7.5 ± 2.2 m^3/s (P=.05, N=20). The net inflow from thermal features above Station B was estimated as 1.5-2.5 m^3/s (20-40% of total non-runoff discharge).

Below Station B the most significant thermal contribution is Ojo Caliente Spring (0.006 m^3/s) (Allen and Day 1935). Sentinel Creek (0.3 m^3/s) receives some thermal water but maintains an average temperature about 10 C lower than the Firehole and so is considered a cold tributary. Nez Perce Creek (2.0 m^3/s) is the last significant tributary to the Firehole and it was generally cooler than the Firehole by 3-5 C. Below Nez Perce the river continued to Madison Junction with no grossly apparent change in discharge.

Temperature

Water temperature at Stations A and B was continuously recorded for all or part of 1974-1977 except for occasional interruptions due to equipment failure or difficulty of access to the recorders during winter. Temperature at other locations was recorded for shorter periods. Air temperature at Old Faithful was obtained for most of the period January, 1975, through September, 1977. Monthly means (average of the daily mean temperatures) of water and air temperature are presented in Figure 7. These same data plus average monthly highs, lows, and extremes are presented in Appendix Tables 5-8.

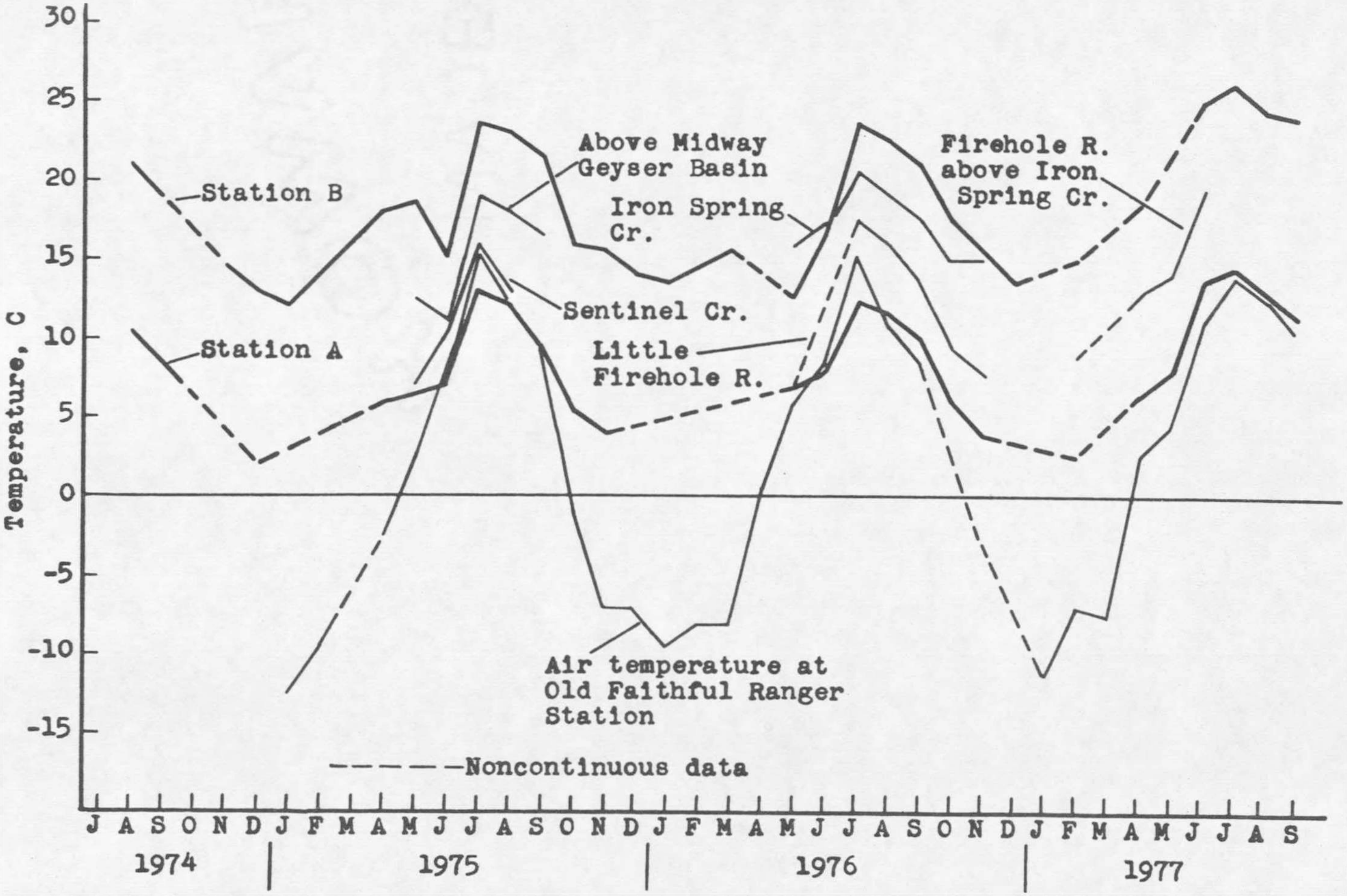

Figure 7. Average monthly mean temperature at indicated locations.

Average monthly mean temperature at Station A ranged from 2.0 C (December, 1974) to 14.5 C (July, 1977). Lower temperatures could have occurred during periods when records were not continuous. This temperature range is typical of mountain streams in this area. Average monthly means at Station B, in contrast, ranged from 12.0 C (January, 1974) to 26.0 C (July, 1977). Station B averaged about 11 C higher than Station A. Highest temperature values recorded during the study period were 20.0 C for Station A and 29.5 C for Station B. These values occurred during the summer of 1977 (Tables 5 and 6).

As earlier stated, Sentinel Creek averaged about 10 C lower than Station B during the late summer. The temperature values recorded above Midway were intermediate between Stations A and B. The Little Firehole averaged about 4 C higher than Station A while Iron Spring Creek was about 8 C higher than Station A. The temperature of the main Firehole just above Iron Spring Creek was intermediate between Stations A and B. Mean monthly air temperature ranged from -12.5 C (January, 1975) to 15.5 C (July, 1975).

Temperature transects of the river indicated that mixing was complete both laterally and vertically except in the vicinity of thermal or cold-water inflows. These exceptions are described in detail under infrared imagery, below.

The periods of high temperature were of the most interest with respect to survival of trout populations and, therefore, the summer months merited additional analysis. Figure 8 presents 5-day averages of mean temperature for Stations A and B. The curves are plotted so that the years 1975-1977 may be directly compared. The 1977 summer temperature (a summer of below-average runoff) was consistently higher than that of 1975 and 1976. This is shown more clearly by Figures 9 and 10 in which are plotted the percentage of days in which the mean temperature equalled or exceeded a given value. These histograms reveal that temperature was significantly higher in June, 1977, and decreasingly so in July, August, and early September (all data are adjusted to correspond to the month of least continuous data).

Figure 11 shows 5-day averages of mean air temperature and Figure 12 shows the percentage of days that mean air temperature equalled or exceeded a given value for the summer months of 1975-1977. June, 1977, was significantly warmer in comparison while July, 1977, was cooler and August and September were only slightly warmer than the same months in 1975 and 1976.

Infrared imagery

IR imagery (obtained 21 October 1976) of the Firehole River from just above Station A to below Nez Perce Creek is presented in Figures 13-20. Although the imagery closely resembles a visible light photograph, it is a record of thermal IR only. Higher temperatures appear as less dense areas in the photographic positives. Thermal features

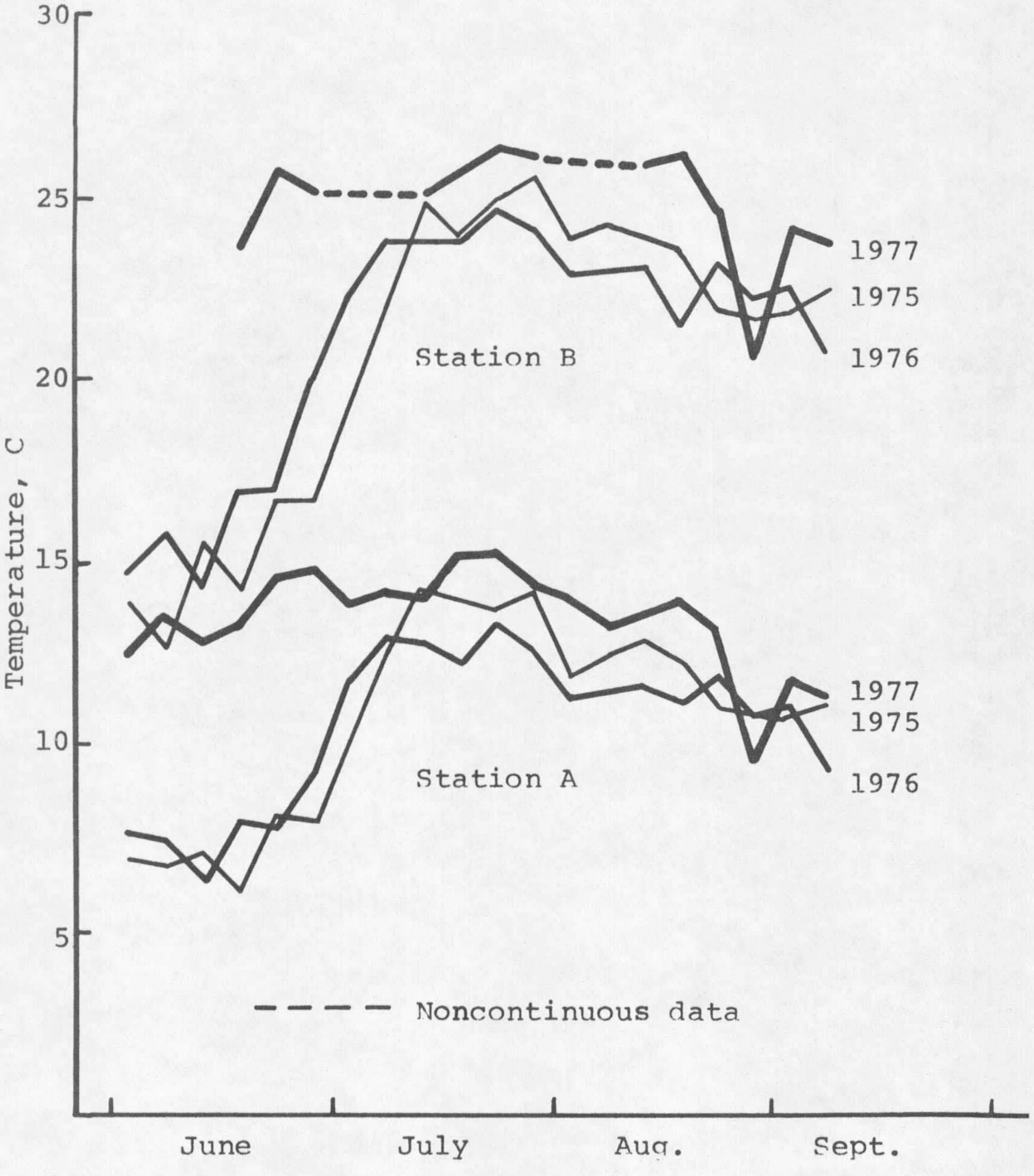

Figure 8. Average 5-day mean temperature for indicated years.

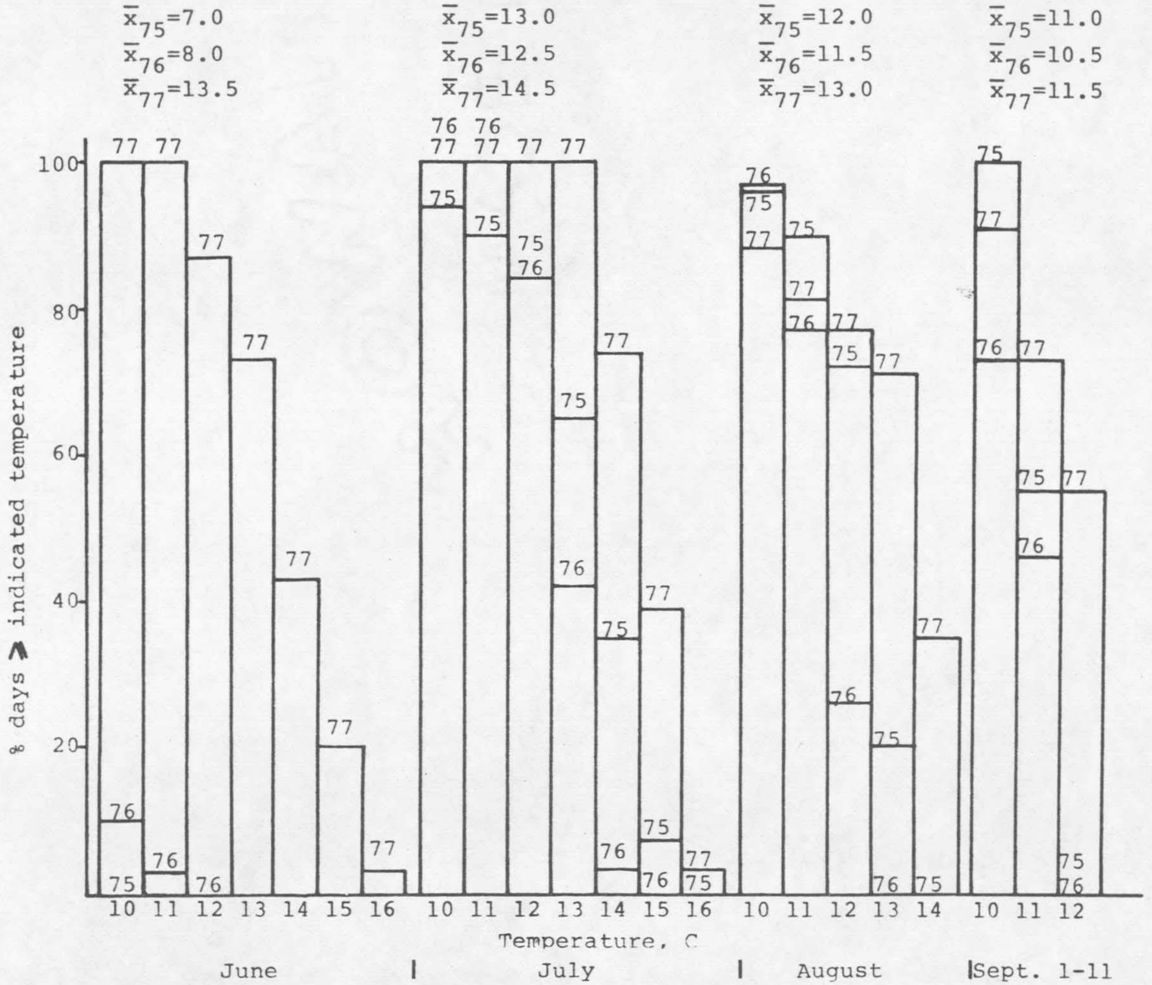

Figure 9. Mean temperature histograms and average monthly means at Station A.

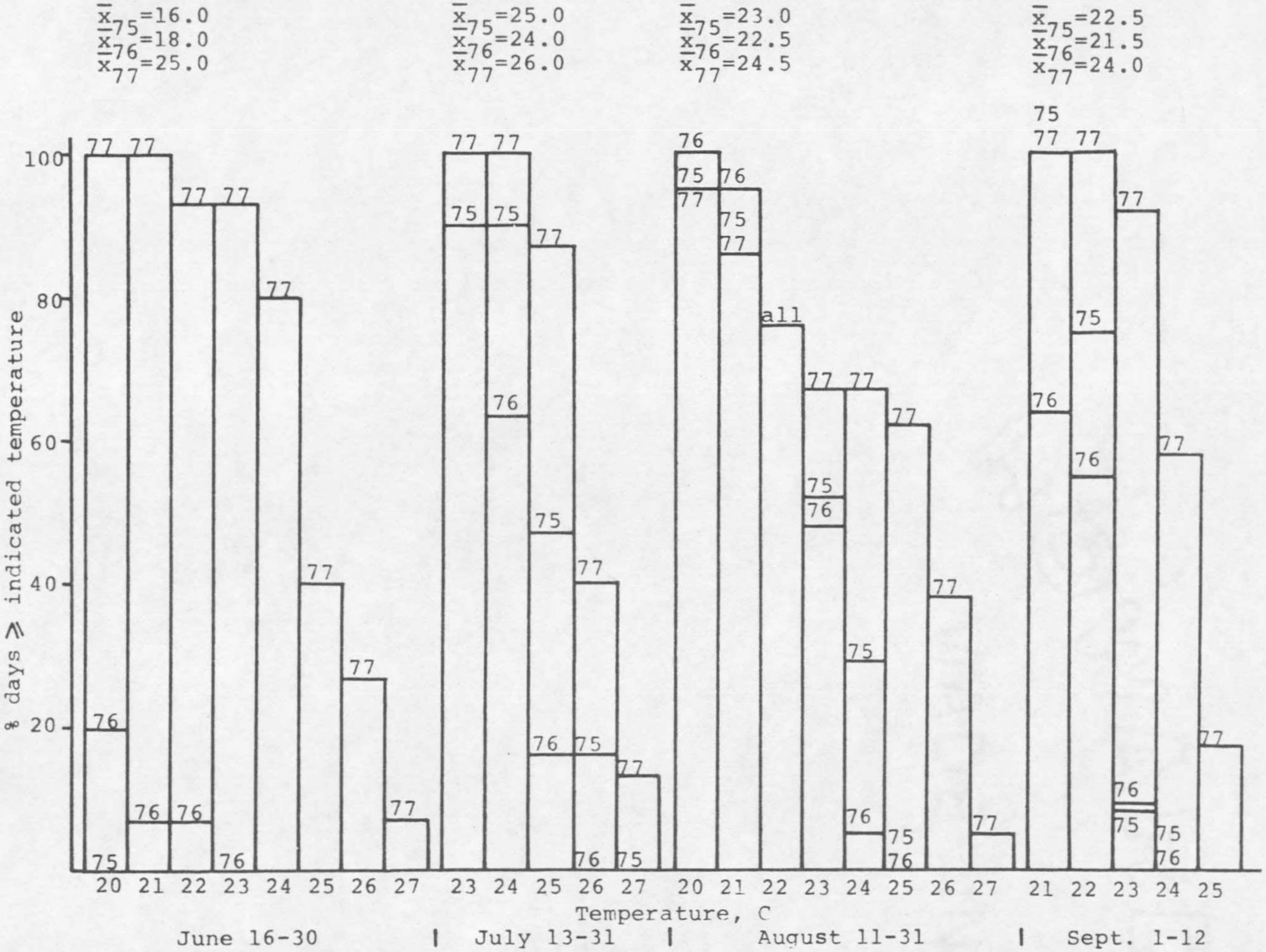

Figure 10. Mean temperature histograms and average monthly means at Station B.

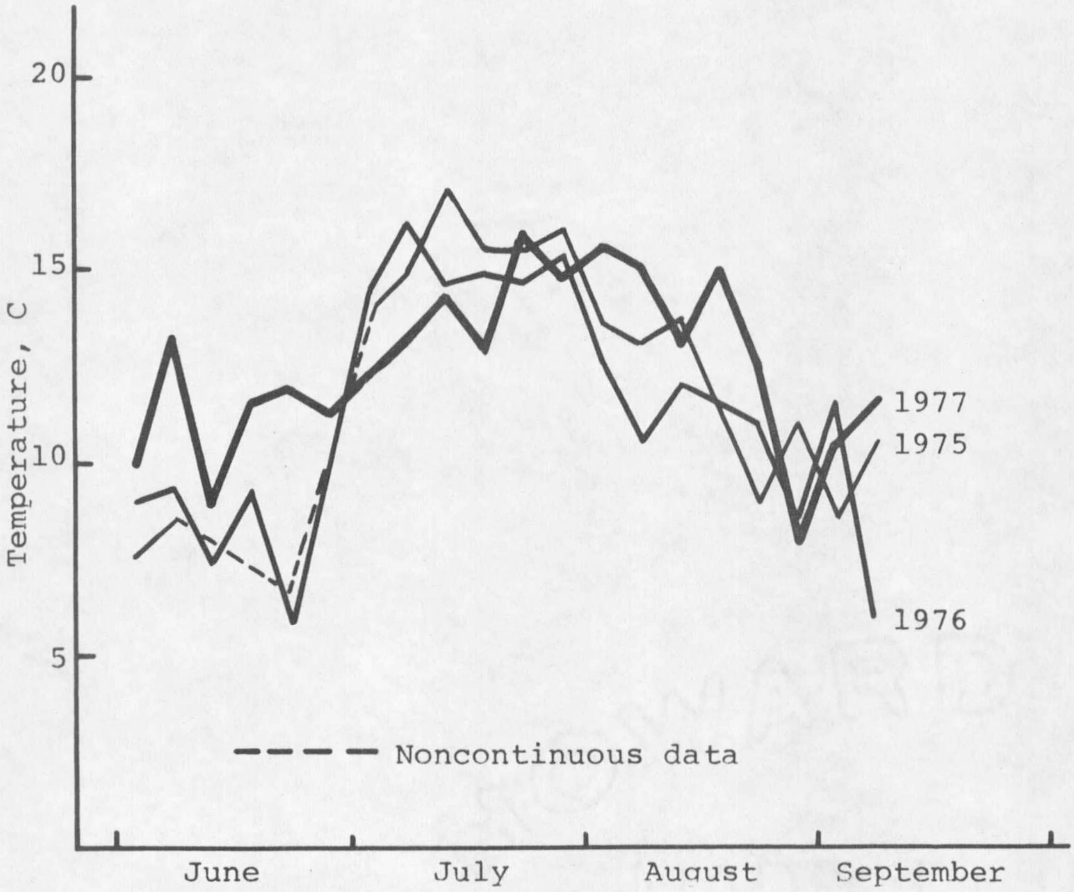

Figure 11. Average 5-day mean air temperatures for indicated years at Old Faithful Ranger Station.

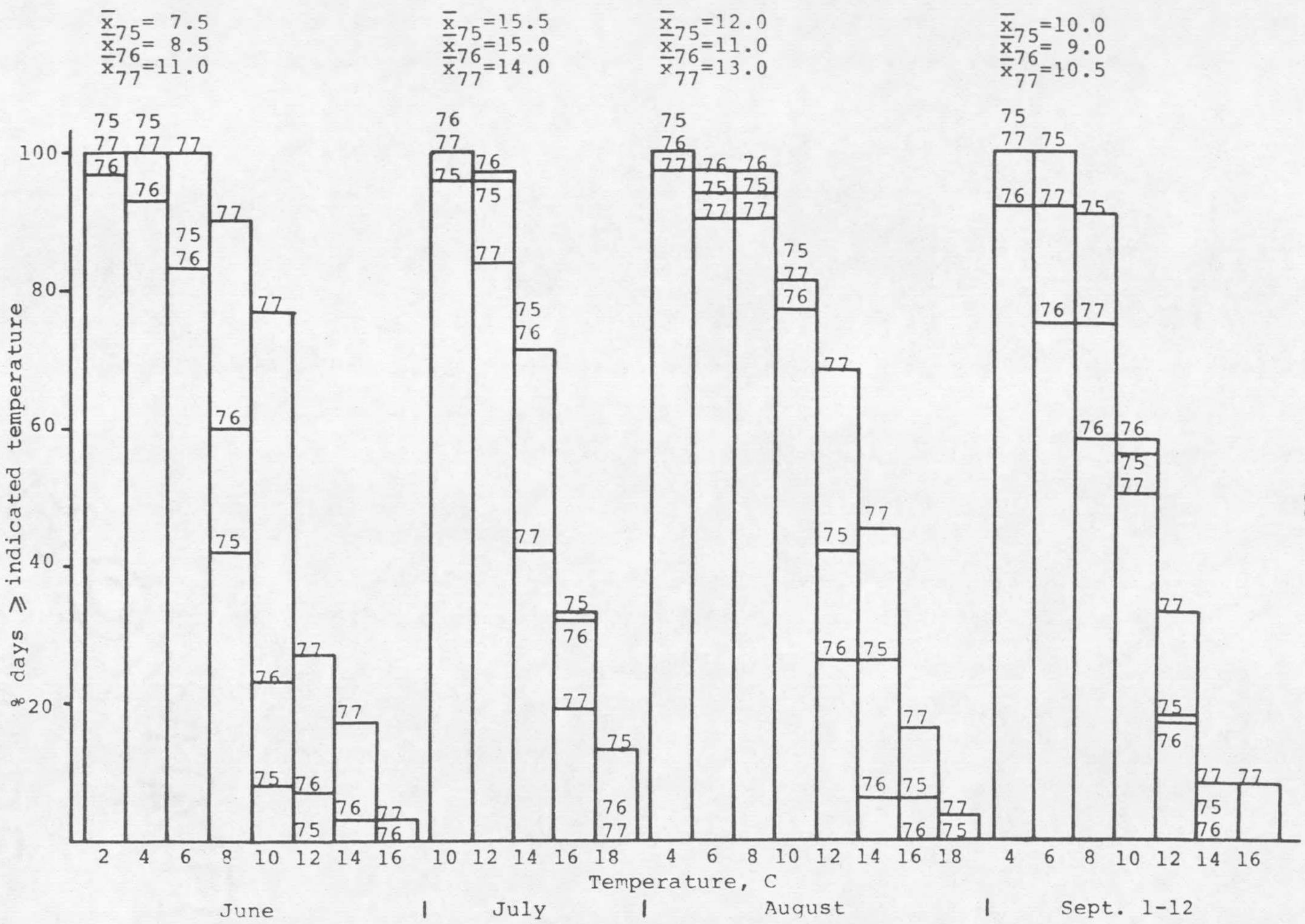

Figure 12. Mean air temperature histograms and monthly average means at Old Faithful Ranger Station.

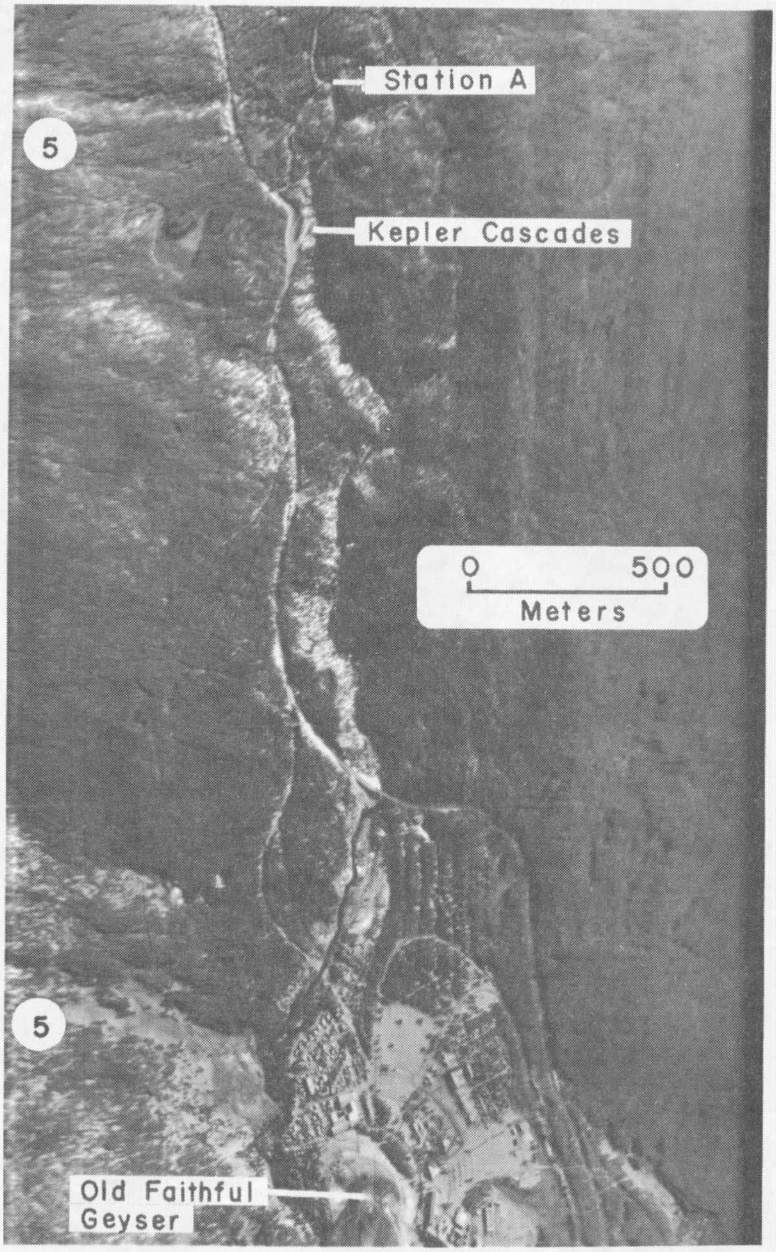

Figure 13. IR imagery of Firehole River from Station A to Old Faithful Geyser. Temperature (C) of river is in left margin; tributary temperature is noted with tributary name. Photographic density is inversely correlated with temperature.

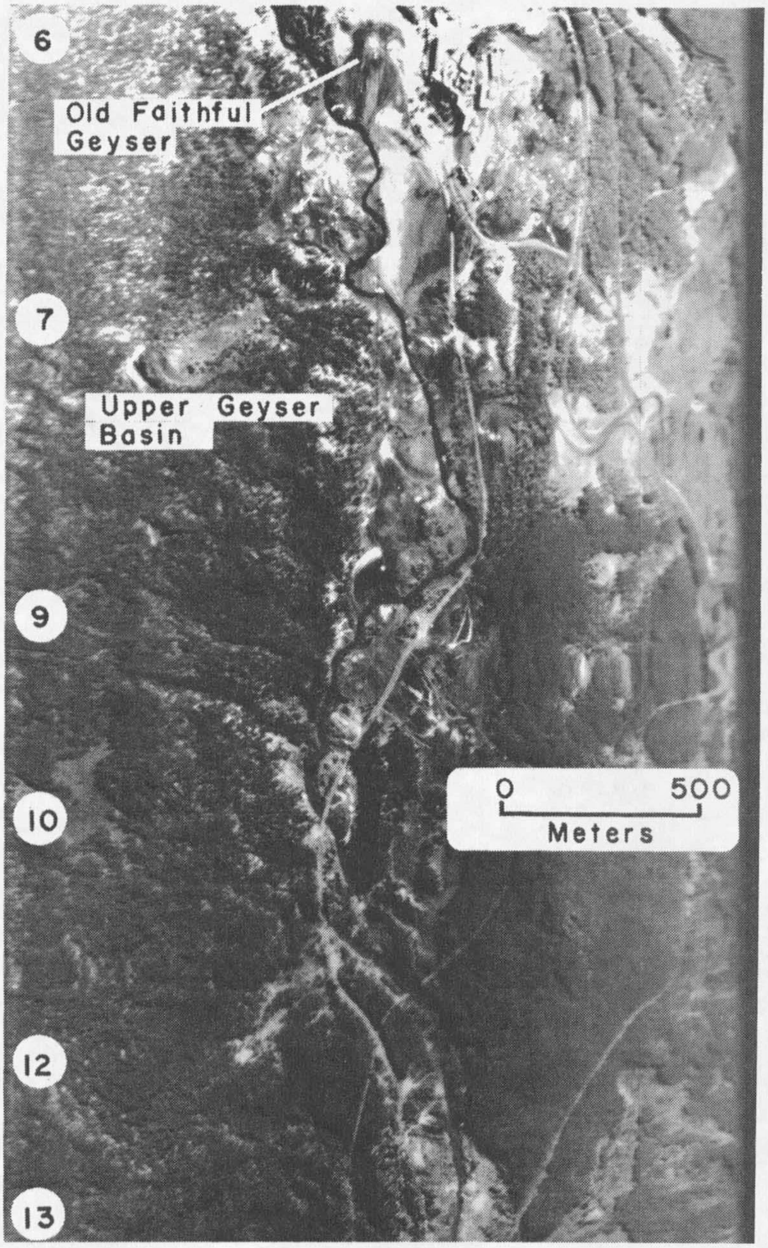

Figure 14. IR imagery of Firehole River in Upper Geyser Basin. Temperature (C) of river is in left margin. Photographic density is inversely correlated with temperature. (Continuous with Figure 13.)

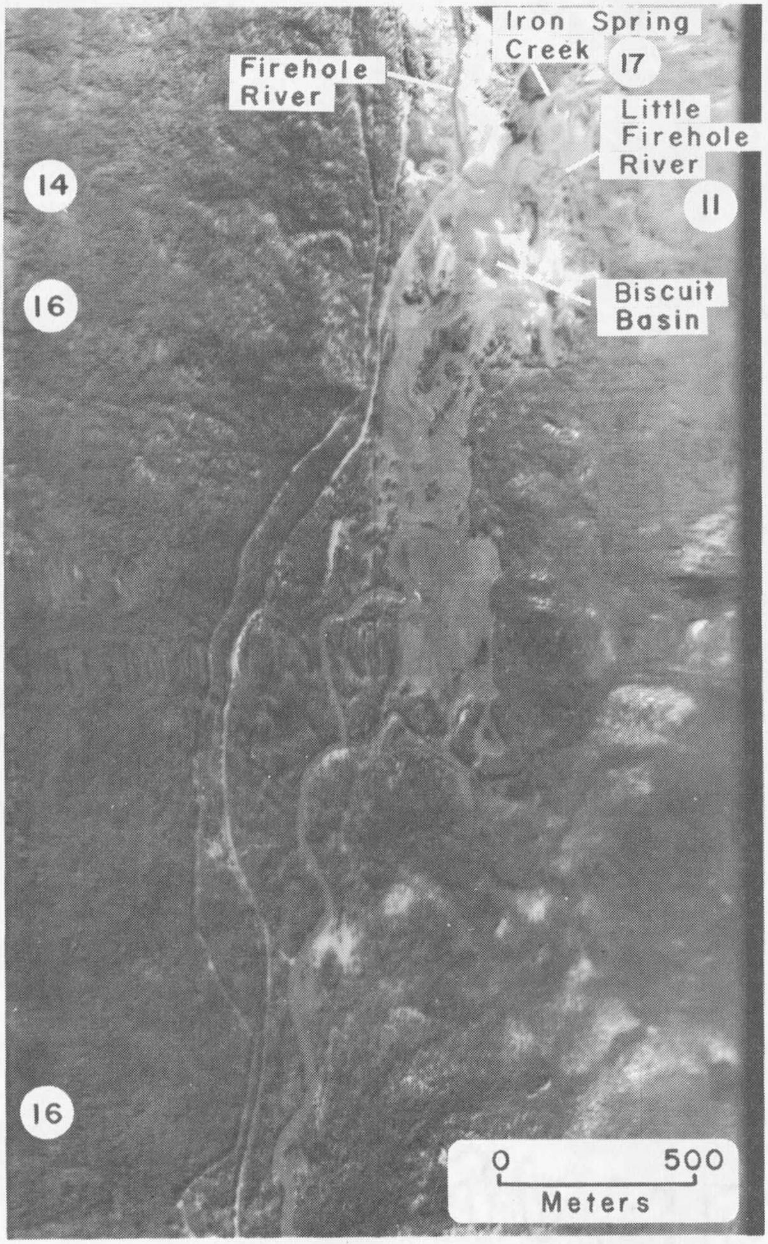

Figure 15. IR imagery of Firehole River below confluence of Iron Spring Creek. Temperature (C) of river is in left margin; tributary temperature is noted with tributary name. Photographic density is inversely correlated with temperature. (Continuous with Figure 14.)

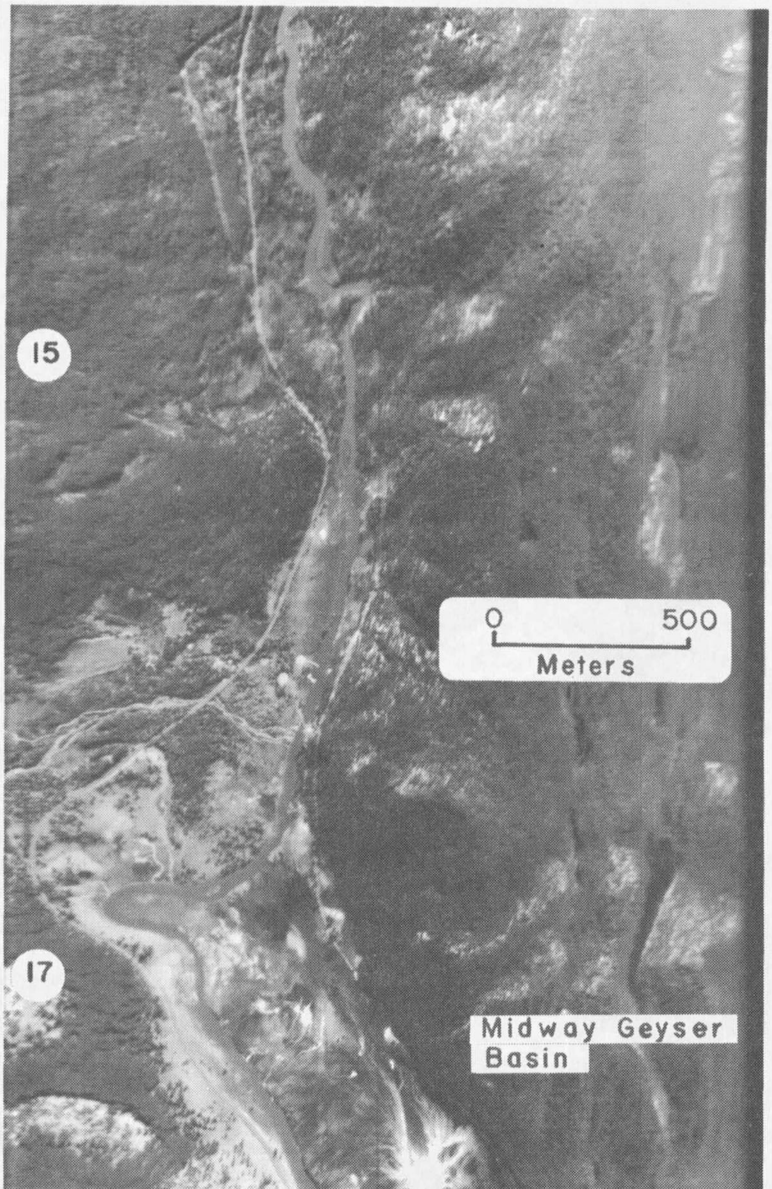

Figure 16. IR imagery of Firehole River entering Midway Geyser Basin. Temperature (C) of river is in left margin. Photographic density is inversely correlated with temperature. (Continuous with Figure 15.)

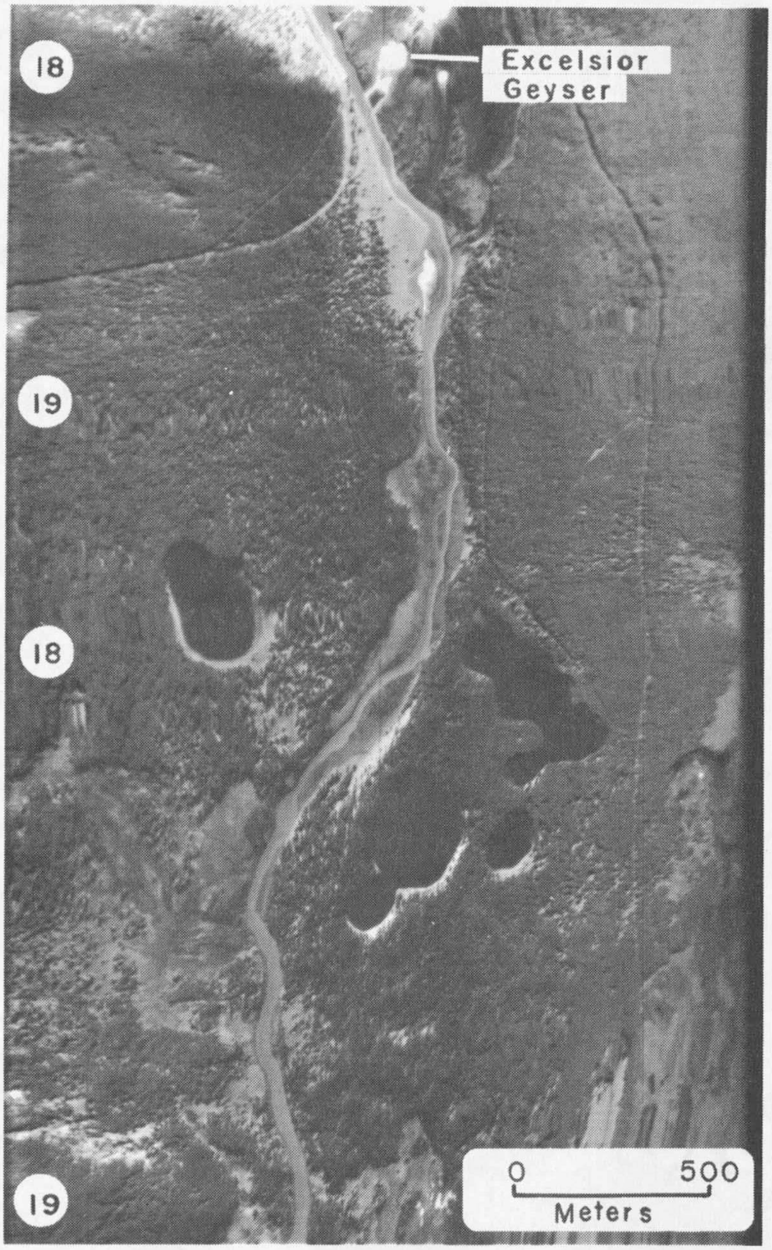

Figure 17. IR imagery of Firehole River below Midway Geyser Basin. Temperature (C) of river is in left margin. Photographic density is inversely correlated with temperature. (Continuous with Figure 16.)

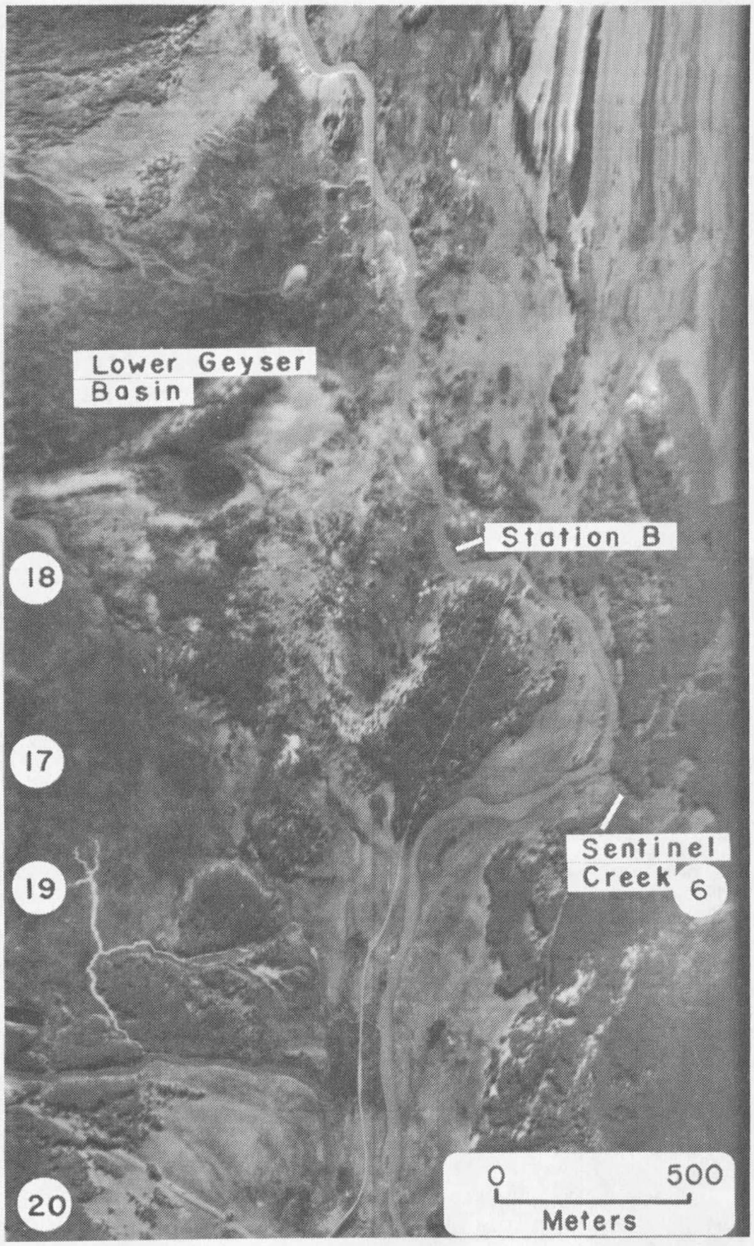

Figure 18. IR imagery of Firehole River in Lower Geyser Basin. Temperature (C) of river is in left margin; tributary temperature is noted with tributary name. Photographic density is inversely correlated with temperature. (Continuous with Figure 17.)

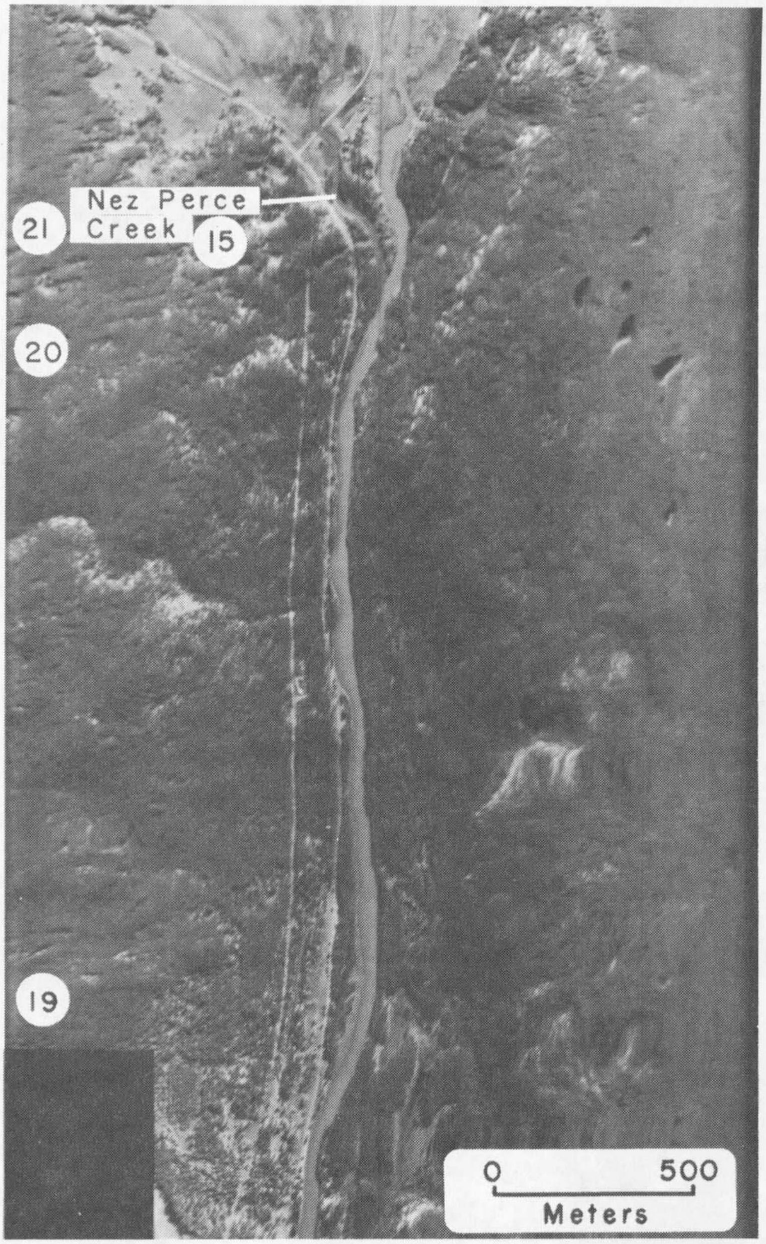

Figure 19. IR imagery of Firehole River at confluence of Nez Perce Creek. Temperature (C) of river is in left margin; tributary temperature is noted with tributary name. Photographic density is inversely correlated with temperature. (Continuous with Figure 18.)

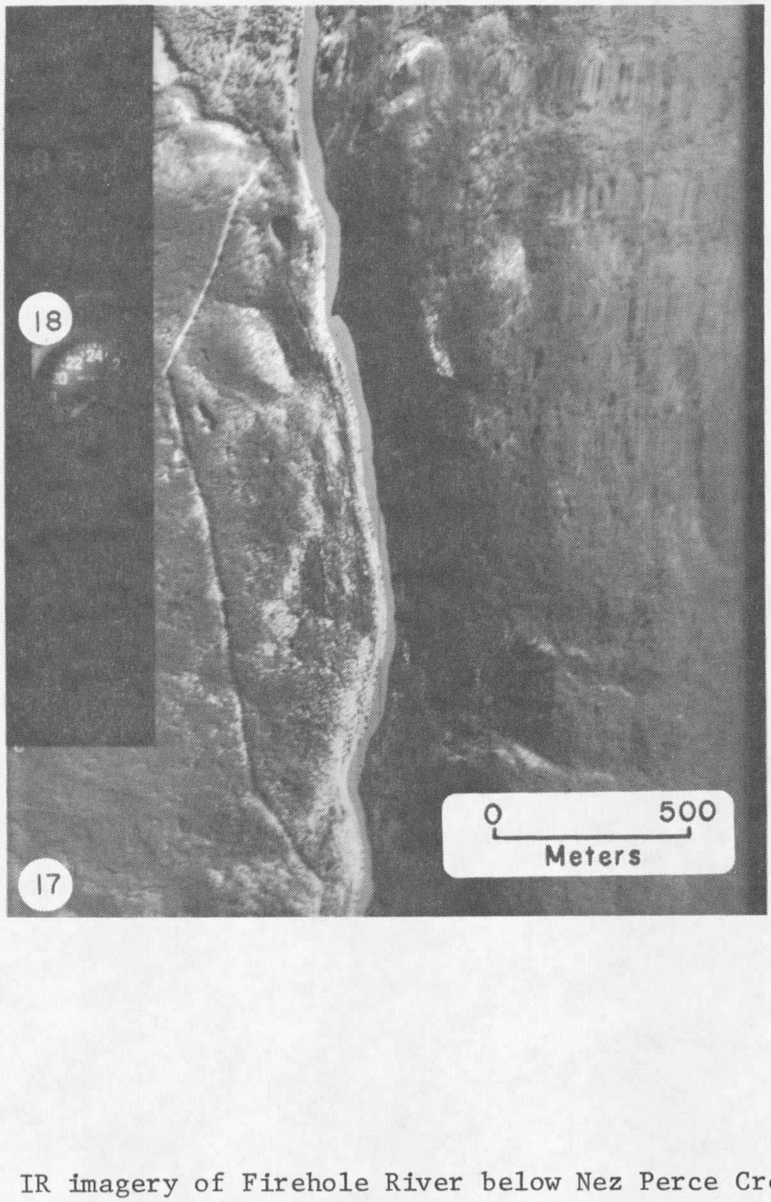

Figure 20. IR imagery of Firehole River below Nez Perce Creek. Temperature (C) of river is in left margin. Photographic density is inversely correlated with temperature. (Continuous with Figure 19.)

appear white; all thermal features appear the same temperature (same density) because the IR equipment was set to the temperature range of the river and saturated at about 27 C. Most thermal features at their sources are considerably warmer than 27 C and, therefore, saturated the IR signal. River and tributary temperatures as determined from the IR imagery are plotted against distance downstream from Station A in Figure 21.

After leaving Station A (temperature, 5 C), the river enters the Upper Geyser Basin and passes Old Faithful Geyser (Figs. 13, 14 and 21). Temperature increased to 14 C just above the confluence with Iron Spring Creek (Figs. 15 and 21). The Little Firehole River (11 C) joins Iron Spring Creek (17 C) which in turn joins the main Firehole resulting in a temperature of 16 C below Biscuit Basin. The river flowed at this temperature until normal decay resulted in a temperature of 15 C at a point above Midway Geyser Basin (Figs. 16 and 21). The temperature rose to 18 C as the river entered Midway Geyser Basin (Figs. 17 and 21) reaching 19 C below Excelsior Geyser. From Excelsior the temperature alternated between 18 and 19 C and was 18 C at Station B (Figs. 18 and 21). The temperature decayed to 17 C at a point just above Sentinel Creek. Below Sentinel Creek (6 C) the temperature increased to 21 C before the confluence of Nez Perce Creek (Figs. 19 and 21). Below Nez Perce (15 C) the temperature decreased

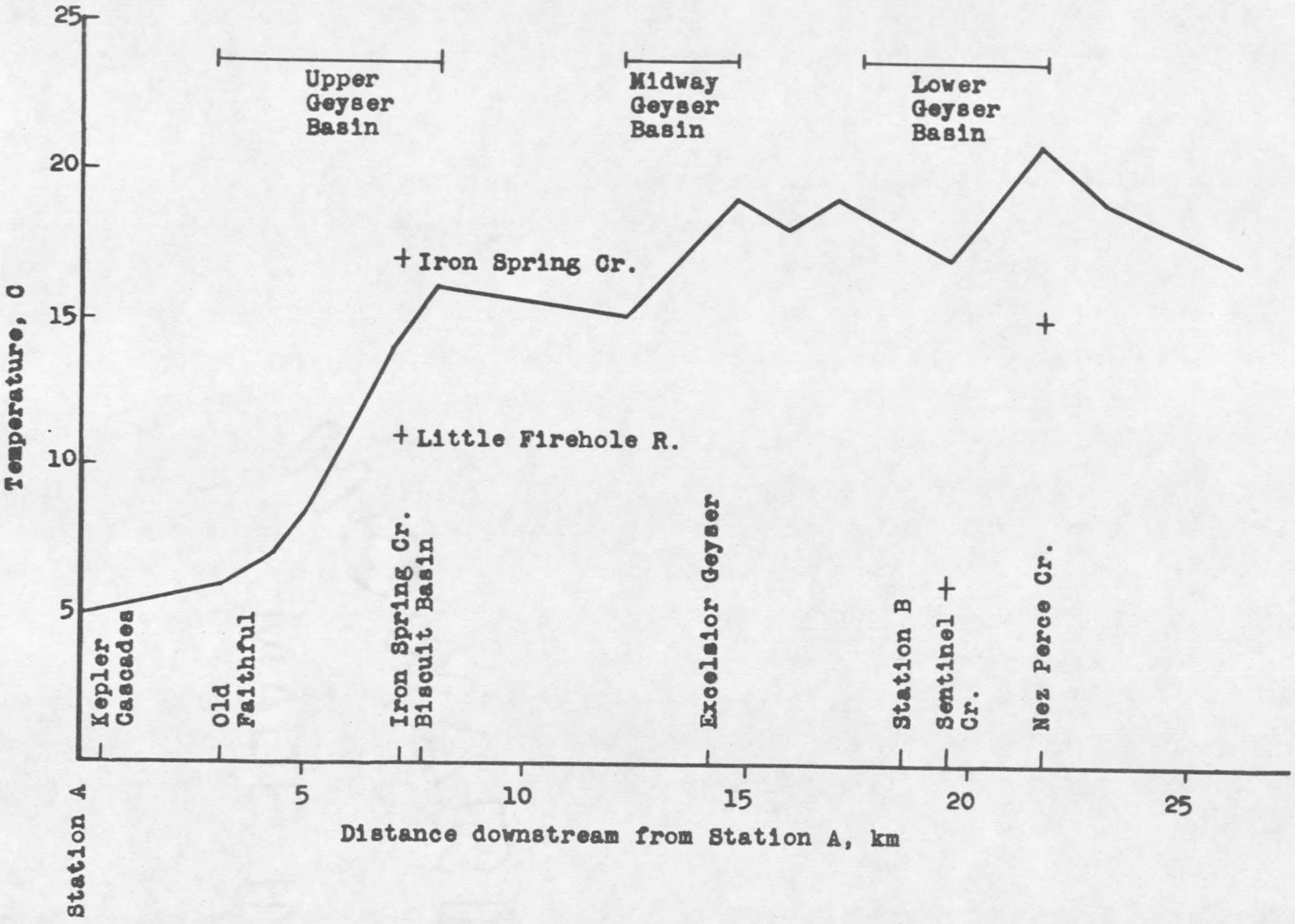

Figure 21. Temperature of Firehole River and tributaries (+) from IR imagery.

to 20 C and then with no further thermal inflows, decayed to 17 C at a point 3.5 km below Nez Perce Creek (Figs. 20 and 21).

Special notice should be made of pronounced thermal gradients (both positive and negative). These occur at the confluence of Iron Spring Creek, Excelsior Geyser, a point in Lower Geyser Basin, and the confluences of Sentinel and Nez Perce Creeks with the Firehole. These areas are shown as photographic enlargements of the imagery (Figs. 22, 24, 27, 29 and 31) and as isotherms constructed from computer printouts (Figs. 23, 25, 26, 28, 30, and 32).

The confluence of Iron Spring Creek and the Firehole is marked by a variety of gradients both positive and negative (Figs. 22 and 23). A gradient is considered positive when the temperature increases from bank to mid-stream or in a downstream direction. Iron Spring Creek (17 C) is joined by the Little Firehole River (11 C) about 100 m upstream from the Firehole. A positive lateral gradient (bank to mid-stream) of 13-17 C was established which was still present at the confluence of the main Firehole (14 C). At this point a second positive gradient of 14-17 C was established. Directly below the confluence both banks were cooler than mid-stream, a condition which was soon degraded by lateral mixing. Small thermal inflows from Biscuit Basin altered the stream temperature for only a short distance. Mixing appeared complete about 400 m below the confluence of Iron Spring Creek when the temperature reached a uniform 16 C.

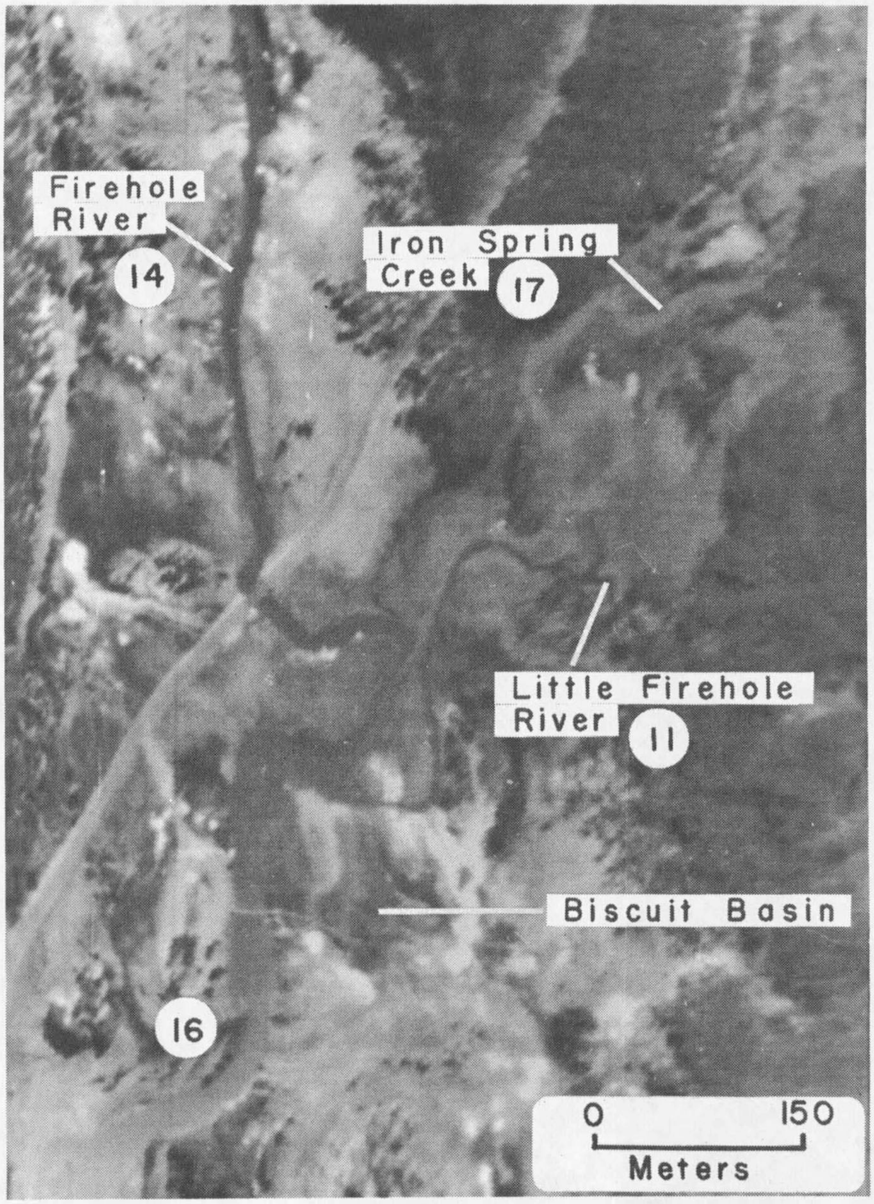

Figure 22. IR imagery of Firehole River at confluence of Iron Spring Creek illustrating thermal gradients. Numbers are temperature (C).

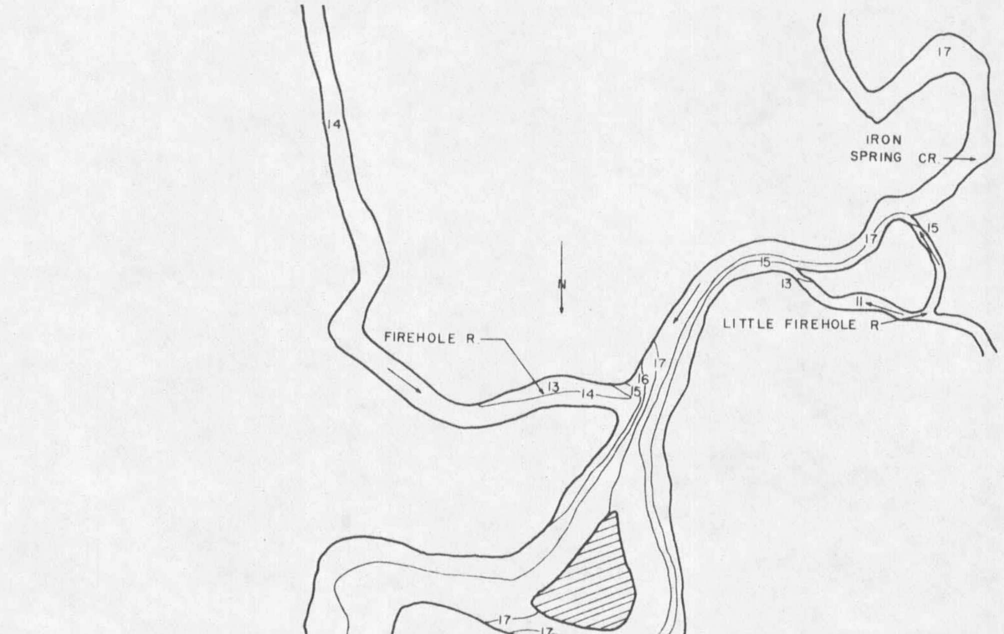

Figure 23. Thermal gradients in Firehole River at confluence of Iron Spring Creek. Isotherms in C. Mid-stream arrows indicate flow direction.

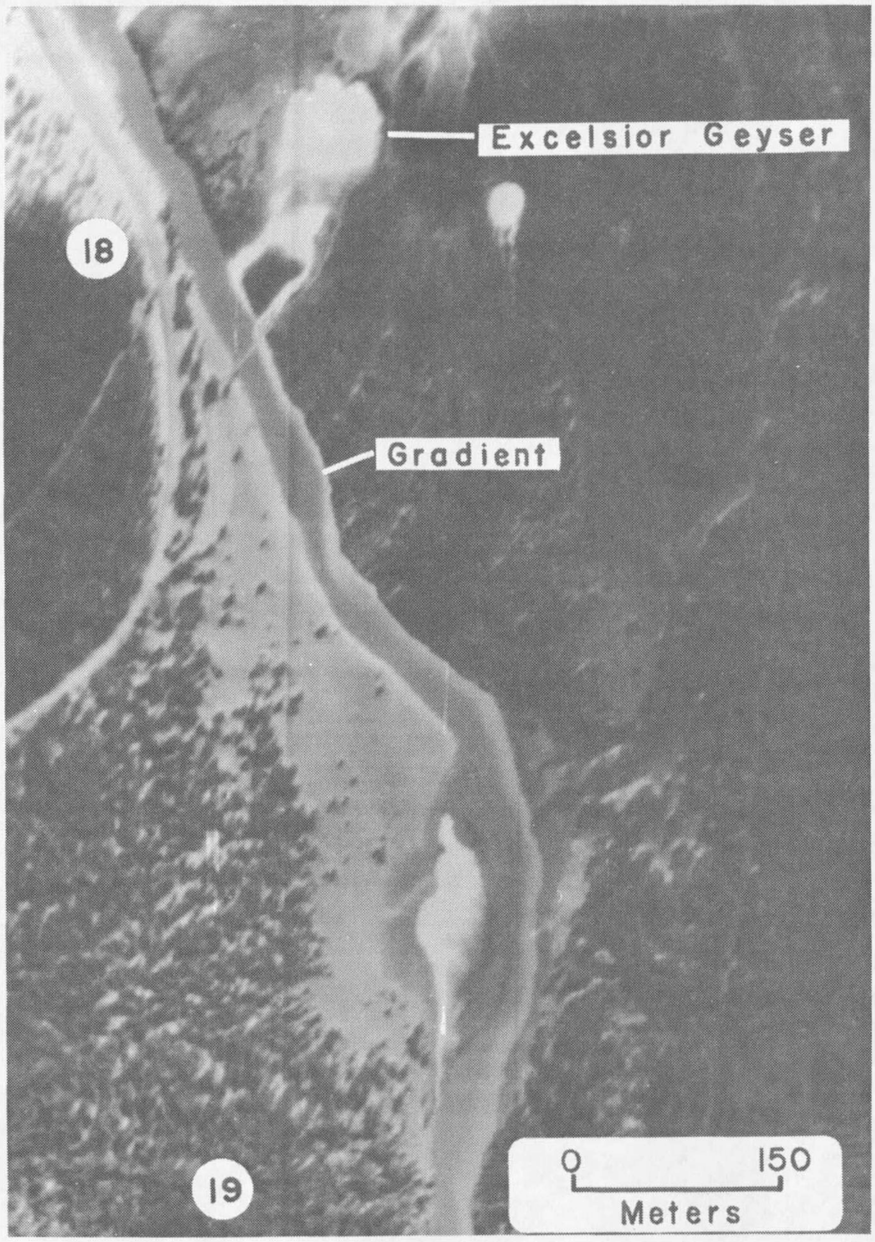

Figure 24. IR imagery of Firehole River at Excelsior Geyser illustrating thermal gradient. Numbers are temperature (C).

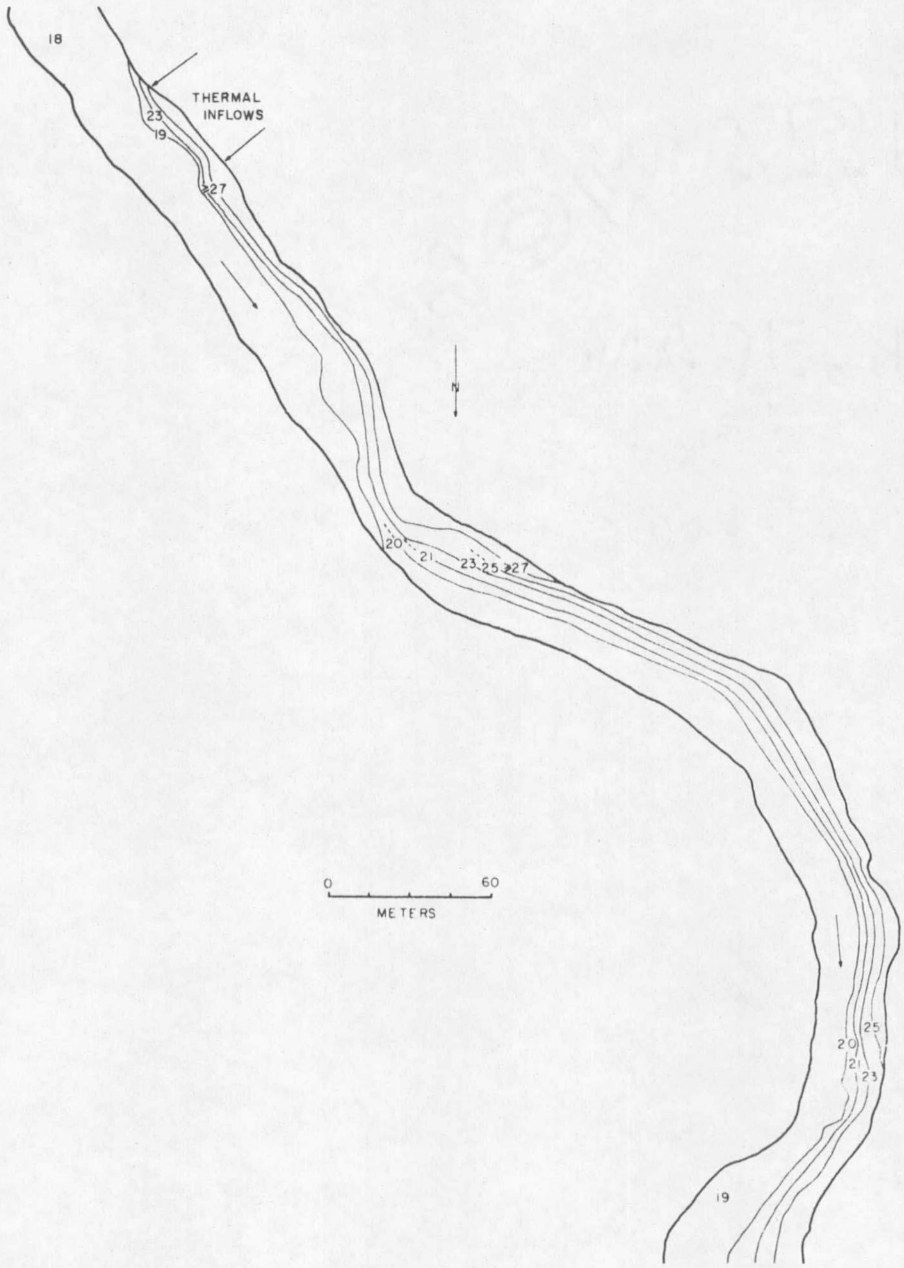

Figure 25. Thermal gradient in Firehole River below inflow of Excelsior Geyser. Isotherms in C. Midstream arrows indicate flow direction.

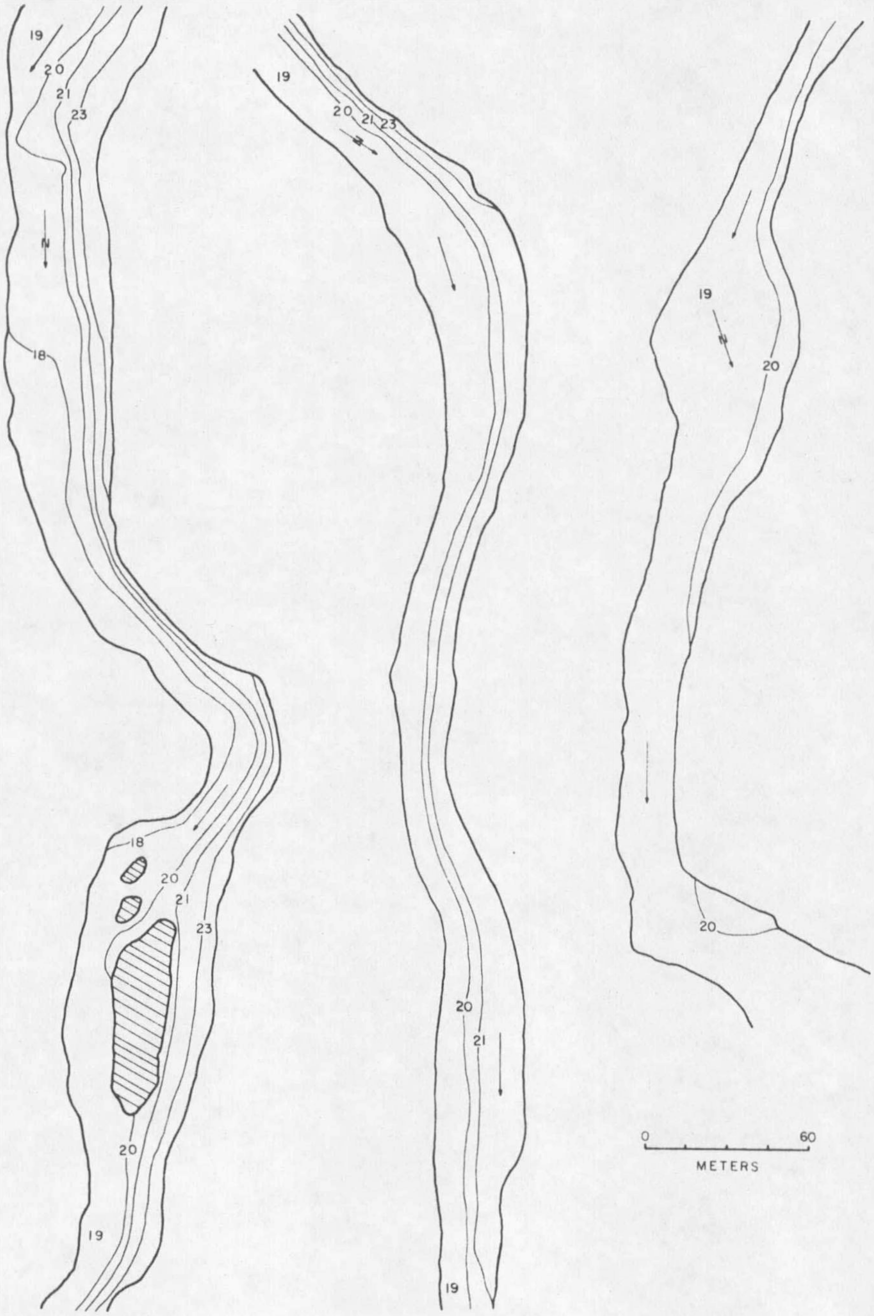

Figure 26. Thermal gradient in Firehole River below Excelsior Geyser. Reaches are continuous l-r and left reach is continuous with Figure 25. Isotherms in C. Mid-stream arrows indicate flow direction

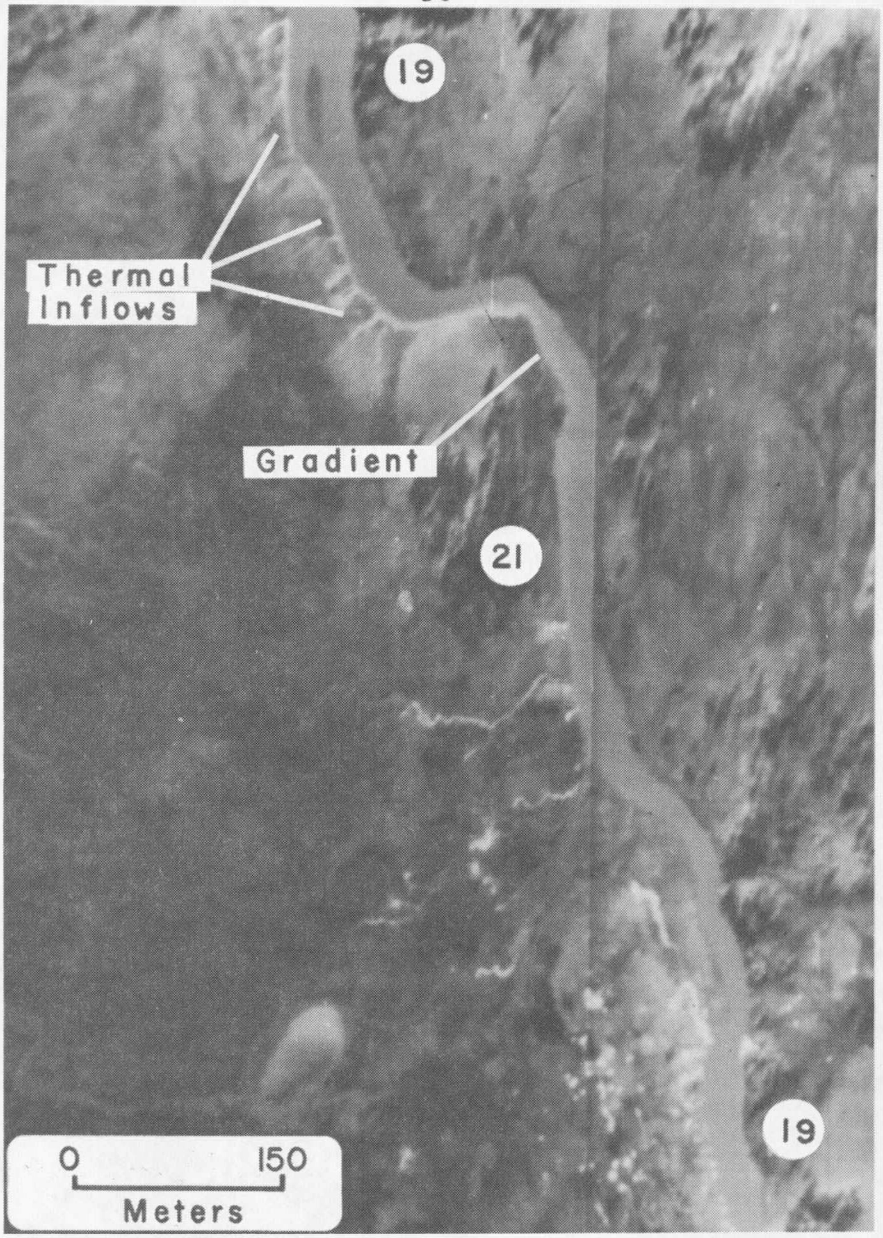

Figure 27. IR imagery of Firehole River at upper end of Lower Geyser Basin illustrating thermal gradient. Numbers are temperature (C).

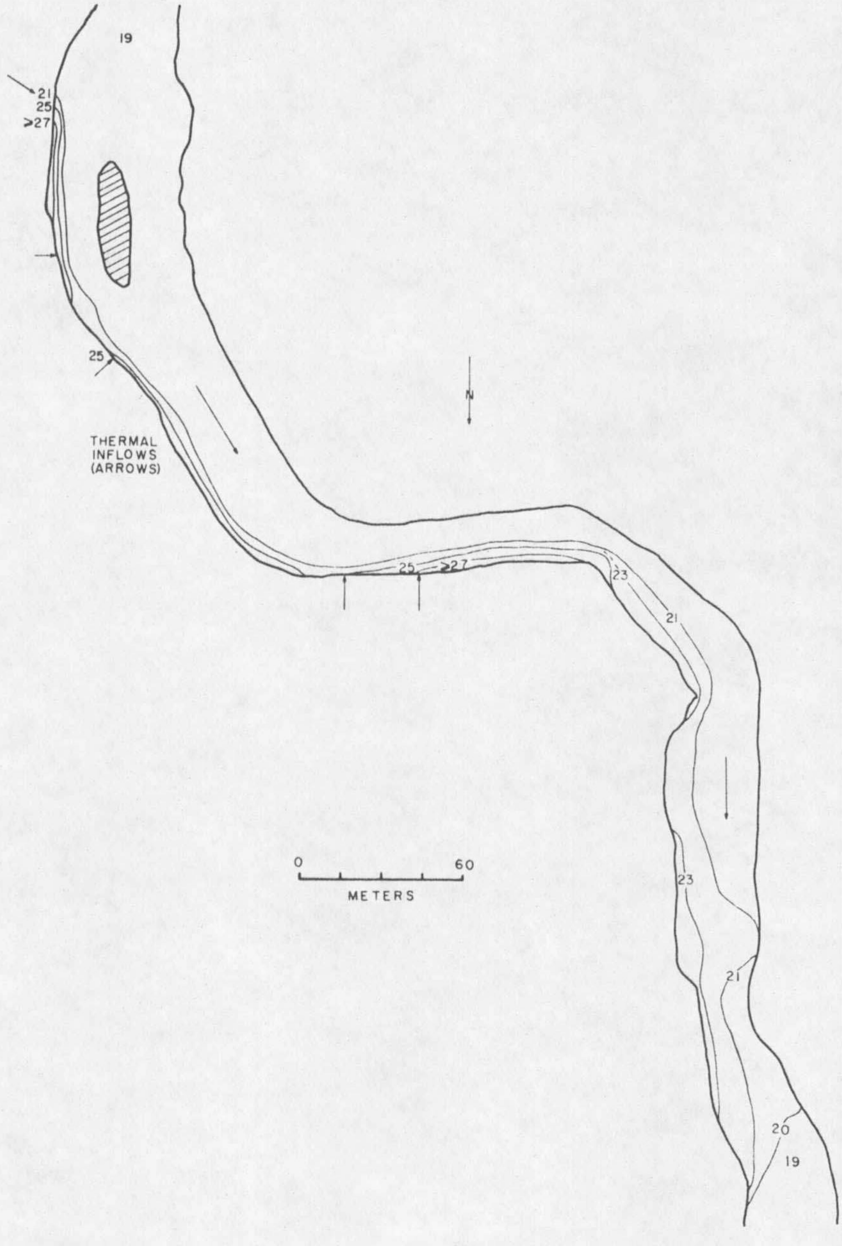

Figure 28. Thermal gradient in Firehole River at upper end of Lower Geyser Basin. Isotherms in C. Mid-stream arrows indicate flow direction.

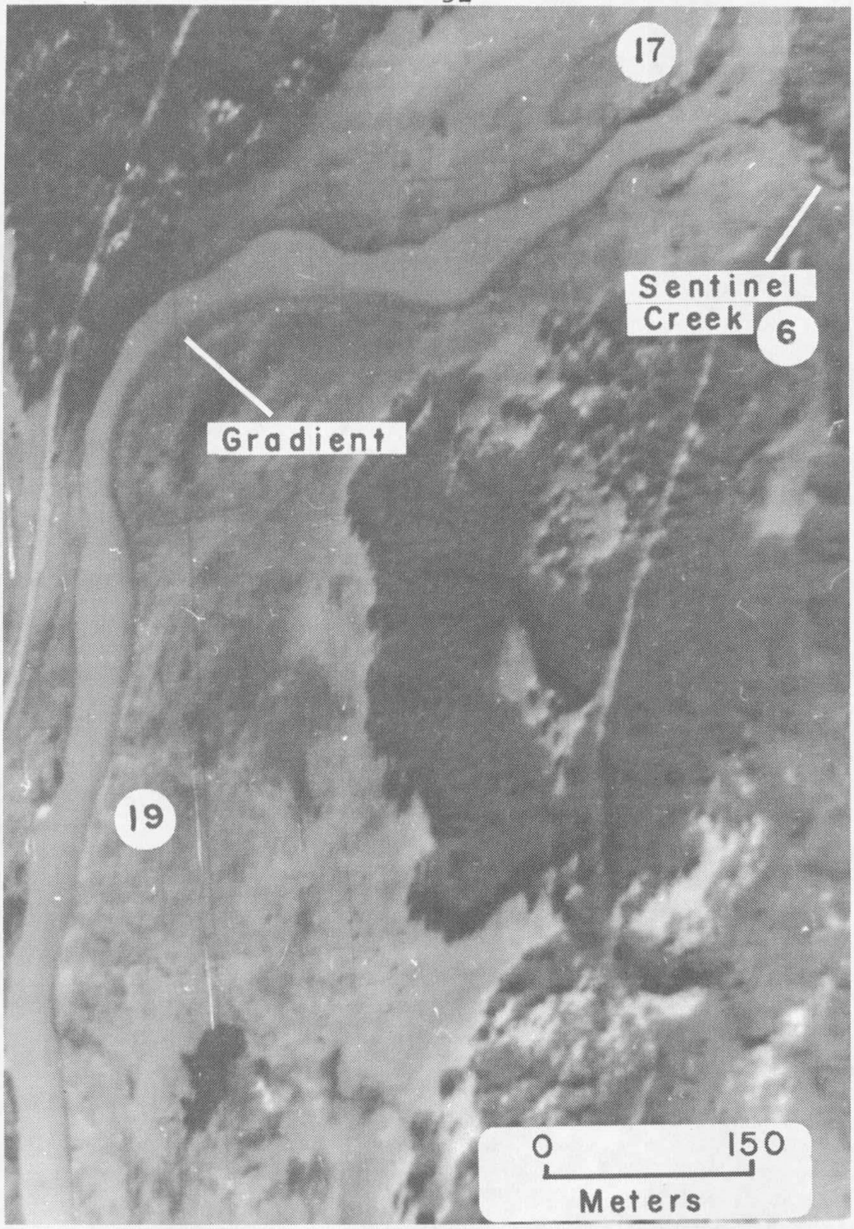

Figure 29. IR imagery of Firehole River at confluence of Sentinel Creek illustrating thermal gradient. Numbers are temperature (C).

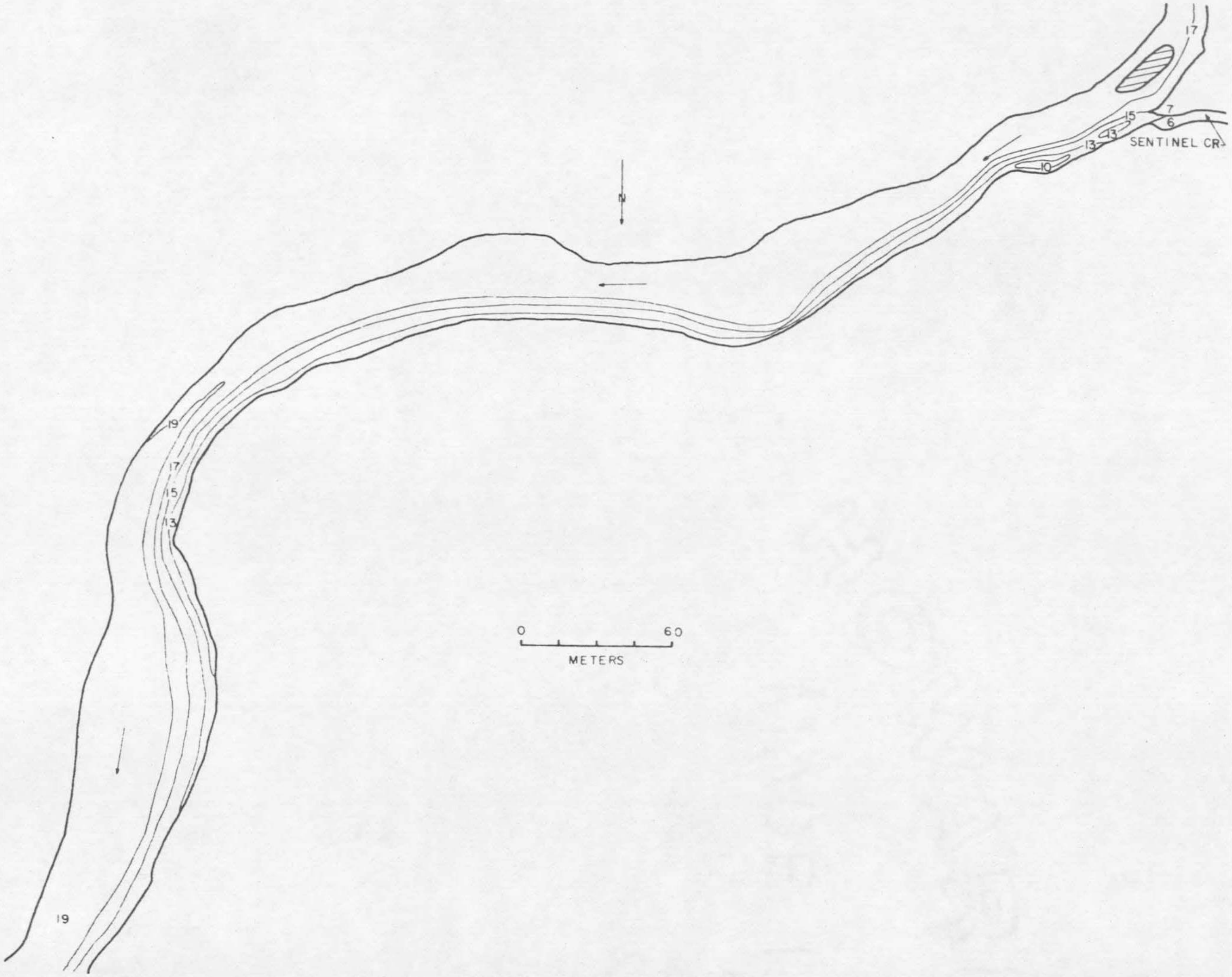

Figure 30. Thermal gradient in Firehole River below Sentinel Creek. Isotherms in C. Midstream arrows indicate flow direction.

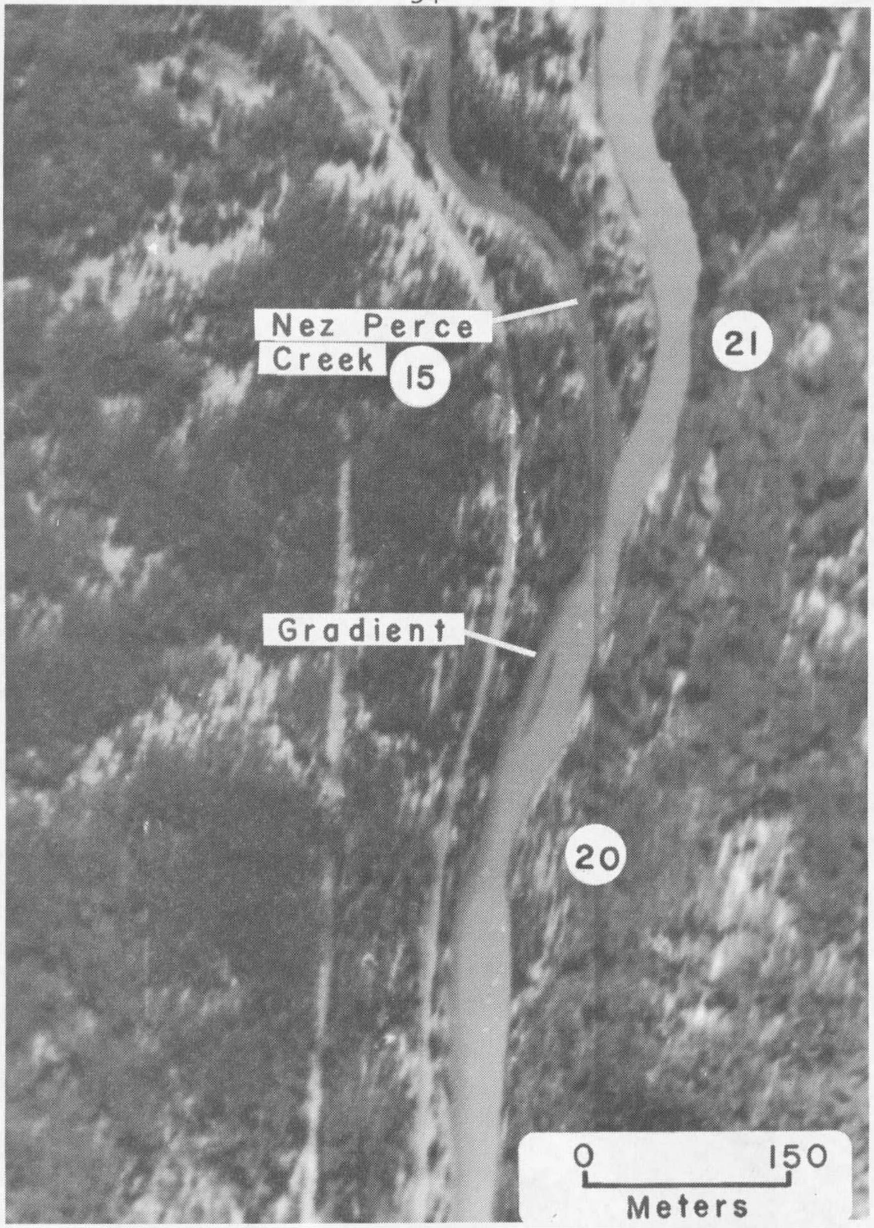

Figure 31. IR imagery of Firehole River at confluence of Nez Perce Creek illustrating thermal gradient. Numbers are temperature (C).

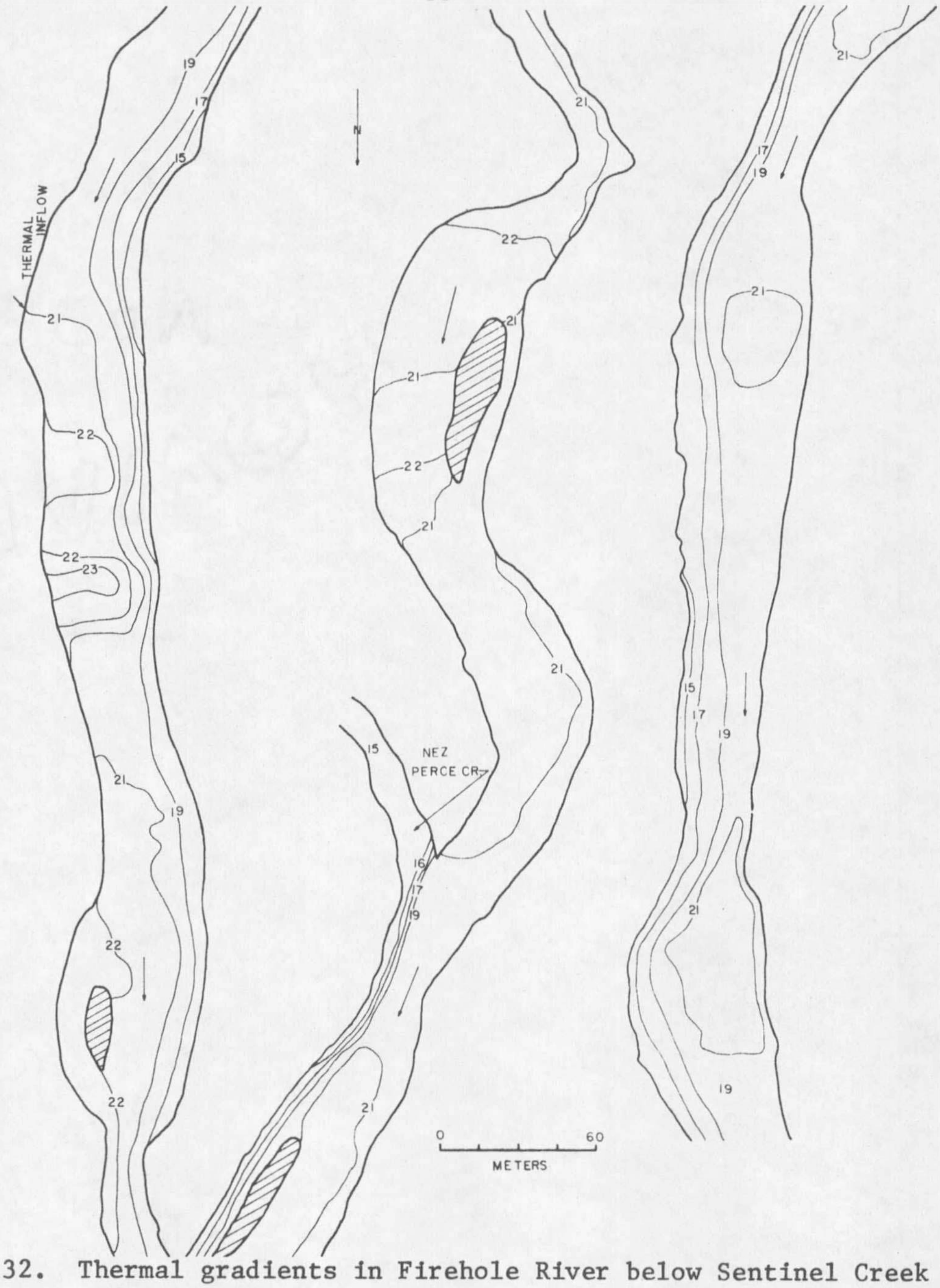

Figure 32. Thermal gradients in Firehole River below Sentinel Creek (1) and below Nez Perce Creek. Reaches are continuous l-r and left reach is continuous with Figure 30. Isotherms in C. Mid-stream arrows indicate flow direction.

The next significant gradient occurred at Midway Geyser Basin with the inflow from Excelsior Geyser (Figs. 24-26). A negative lateral gradient of 27-18 C (as earlier mentioned the IR equipment saturated at 27 C) occurred below Excelsior Geyser which degraded slowly by lateral mixing and disappeared about 1.8 km downstream at a temperature of 19 C. This gradient persisted downstream much farther than concluded by Argyle (1966). He assumed degradation of the gradient occurred within a 300 m reach below the lower Excelsior Geyser inflow although his data indicated a gradient very similar to that found in the present study.

The next gradient occurred at an area near the beginning of Lower Geyser Basin (Figs. 27 and 28). A negative gradient of 27-19 C occurred due to thermal springs along the bank. This gradient decayed over a reach of about 500 m when the temperature stabilized at 19 C.

The most interesting gradient, from the aspect of its influence on resident trout populations (Kaya et al. 1977), occurred at the confluence of the cold tributary, Sentinel Creek (Figs. 29, 30, and 32). As Sentinel Creek (6 C) entered the Firehole (16-17 C) a positive lateral gradient of about 7-17 C occurred. This gradient decayed to 13-19 C about 500 m downstream. With downstream flow the west bank warmed due to lateral mixing. At the same time the east bank warmed from thermal influences (some visible and some possibly submerged) and possibly from solar heating of the somewhat shallower depths in this reach. The gradient established by the confluence of Sentinel Creek persisted for about 1 km downstream (about 600 m above Nez Perce Creek). The temperature approached a uniform 21 C just above Nez Perce Creek (15 C). At Nez Perce Creek (Figs. 31 and 32) a positive gradient of 15-19 C was established which decayed over a reach exceeding 500 m.

Heat rate from geothermal inflows

An estimate of the thermal power added to the Firehole River by thermal inflows can be made by assuming that the river is thermally homogeneous (i. e. in the absence of thermal influences no longitudinal temperature gradient would exist at a given point in time) between Stations A and B. Any temperature differences, at the same point in time, would then be due entirely to thermal additions. This assumption is believed reasonable since the ambient conditions are comparable at Stations A and B. Increased water temperatures normally associated with downstream flow would be offset by greater average depth in the lower reaches, a factor which would tend to reduce the heat exchange that would normally result from the somewhat higher air temperatures and less shading found there.

The temperature that water would enter the Firehole from all sources in the absence of geothermal heating was assumed to be that of the river at Station A. The heat rate due to thermal inflows above any given point was calculated as the product of the discharge at that point, the temperature difference between that point and Station A, and the specific heat of water. From these calculations the average power added by thermal inflows (during non-runoff periods) was: Upper Geyser Basin (not including Iron Spring Creek), 59.7 ± 14.2 MW (P=.05, N=6); Iron Spring Creek, 80.2 ± 19.4 MW (P=.05, N=8); Firehole River between Stations A and B, 303 ± 59 MW (P=.05, N=16).

The above values do not account for heat lost due to excess temperature decay. An estimate of this decay may be made for the river between Stations A and B by observing the behavior of temperature from Biscuit Basin to above Midway Geyser Basin and downstream from Nez Perce Creek (these reaches have little or no geothermal inflow and continuous temperature decay may be observed within the reaches; Figs. 15, 16, and 19-21). These observations were made on a day of average climatic conditions with calm winds, air temperature above freezing, and clear skies. The average temperature decay in these reaches was about 0.5 C/km. This decay rate multiplied by 18.5 km (distance between Stations A and B) and then by a discharge of 3.16 m^3/s (average non-runoff discharge at Station B divided by two) results in an estimated 122 MW of power dissipated between Stations A and B. If this is added to the previously calculated value of 303 MW, the total heat rate due to geothermal inflows between Stations A and B was approximately 425 MW. No compensation could be made for possible influent reaches where heat could be lost to the groundwater. Interestingly, Allen and Day (1935) estimated 448.5 MW for the same reach of river by measuring the heat rate for each individual thermal feature.

Solar insolation

Solar insolation for the summers of 1976-1977 is plotted as 5-day averages in Figure 33 and as monthly histograms in Figure 34. The monthly mean insolations are shown in Table 3 compared with calculated clear-sky insolation and with values estimated from Bennett (1965) who presents average monthly insolation maps for the United States prepared from long-term measurements at numerous locations. Clear-sky values were calculated using angular relationships of the earth and sun and assuming that the average, monthly, clear-sky power was present daily (i.e. cloudless days). The daily energies and clear-sky powers measured at the Old Faithful Ranger Station are presented in Appendix Tables 9 and 10.

Comparative insolations for the two summers were: May 14-31 of 1976, greater by 15.5%; June of 1976, less by 1.5%; July of 1976, greater by 2.9%; August of 1976, greater by 11.1%; September 1-12 of 1976, less by 15.4%; overall, summer of 1976, greater by 2.2% (a difference which is not significant when the ±5% accuracy of the solarimeter is considered). The measured monthly insolation ranged

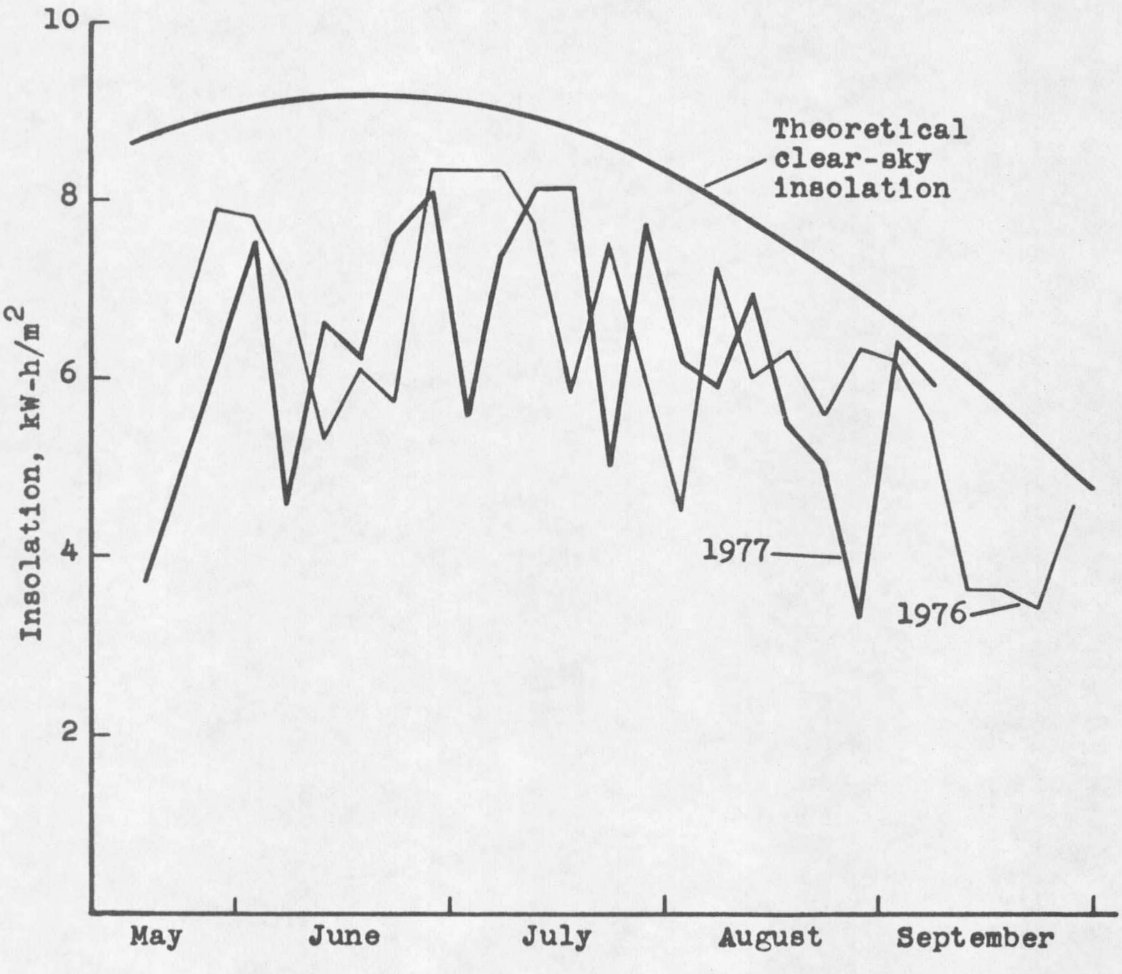

Figure 33. Total daily insolation (averaged over 5-day periods) from sun and sky on a horizontal surface at Old Faithful Ranger Station.

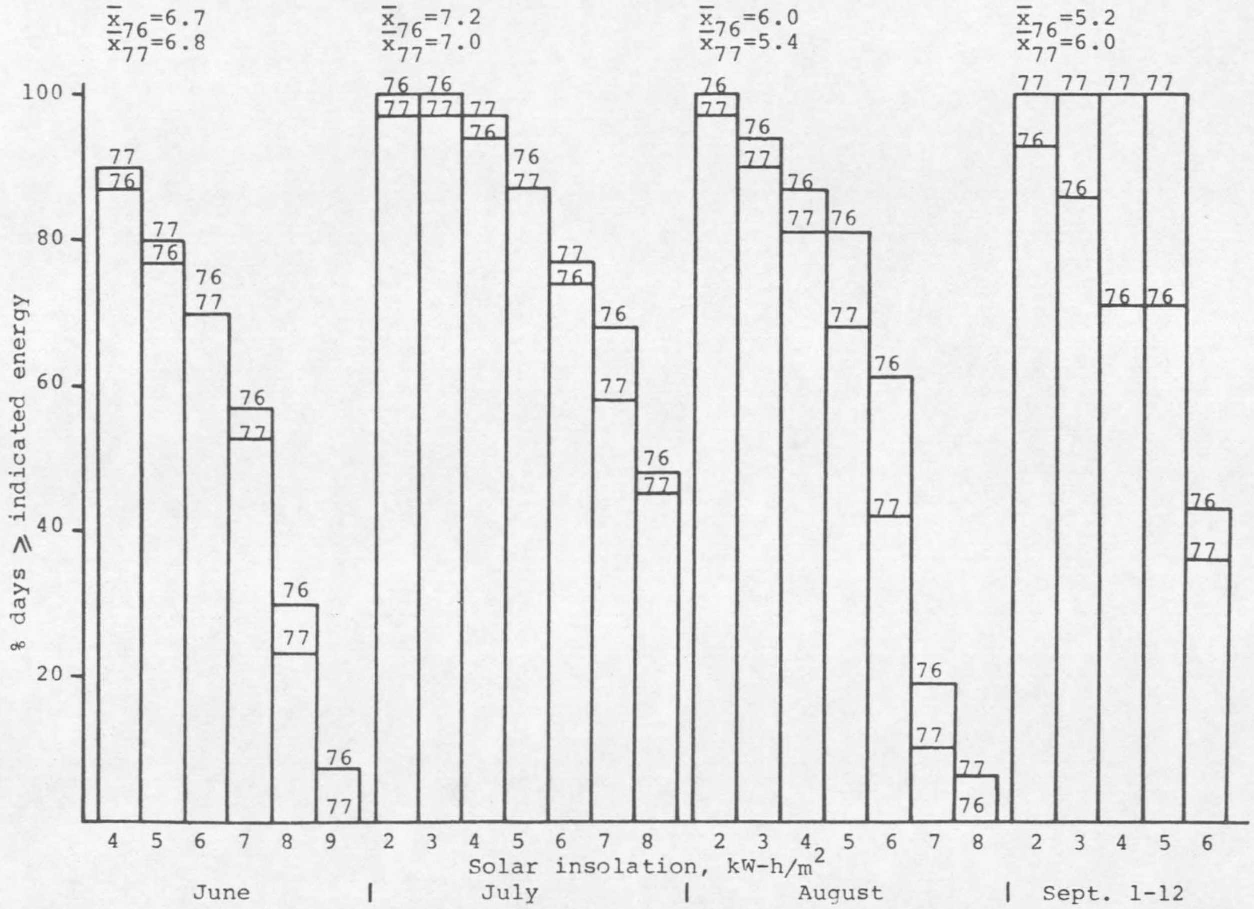

Figure 34. Daily solar insolation histograms and monthly averages at Old Faithful Ranger Station. Abscissa is solar energy from sun and sky on a horizontal surface.

Table 3. Mean daily insolation ($\overline{E}_m$) measured at Old Faithful Ranger Station compared with mean calculated clear-sky insolation ($\overline{E}_c$) and values estimated from Bennett (1965).

Month	Days	Year	$\overline{E}_m$ ($kW\text{-}h/m^2$)	$\overline{E}_c$ ($kW\text{-}h/m^2$)	$\overline{E}_m/\overline{E}_c$	Bennett (1965) ($kW\text{-}h/m^2$)
May	23-31	1976	6.7	8.9	0.75	6.7
		1977	5.8		0.65	
June	1-30	1976	6.7	9.1	0.73	7.6
		1977	6.8		0.75	
July	1-31	1976	7.2	8.8	0.82	7.6
		1977	7.0		0.80	
Aug.	1-31	1976	6.0	7.6	0.79	6.7
		1977	5.4		0.71	
Sept.	1-14	1976	5.2	6.4	0.81	5.2
		1977	6.0		0.94	

from 65-94% of calculated clear-sky energy and these values were generally lower than those from Bennett (1965) (Table 3). These measured values appear reasonable as Bennett's measurements were, in general, from lower dryer elevations.

The thermal loading between Stations A and B from solar insolation (Table 4) was calculated as the product of the mean, monthly insolation and the river surface area (383,980 m^2, obtained by planimetering the IR imagery). The loadings for June through August were calculated from the measured insolation averaged for 1976 and 1977. The loads for the remaining months (when no or incomplete data were

Table 4. Mean monthly power added to Firehole River between Stations A and B from solar insolation ($\overline{E}_s$) and geothermal inflows ($\overline{E}_g$) and the ratios $\overline{E}_s/\overline{E}_g$, $\overline{E}_s/(\overline{E}_s+\overline{E}_g)$ and $\overline{E}_g/(\overline{E}_s+\overline{E}_g)$.

Month	$\overline{E}_s$ (MW)	$\overline{E}_g$ [2] (MW)	$\overline{E}_s/\overline{E}_g$ (%)	$\overline{E}_s/(\overline{E}_s+\overline{E}_g)$ (%)	$\overline{E}_g/(\overline{E}_s+\overline{E}_g)$ (%)
January	31	425	7.3	6.8	93.2
February	44	"	10.4	9.4	90.6
March	64	"	15.1	13.1	86.9
April	85	"	20.0	16.7	83.3
May	101	"	23.8	19.2	80.8
June[1]	103	"	24.2	19.5	80.5
July[1]	108	"	25.4	20.3	79.7
August[1]	87	"	20.5	17.0	83.0
September	70	"	16.5	14.1	85.9
October	49	"	11.5	10.3	89.7
November	33	"	7.8	7.2	92.8
December	26	"	6.1	5.8	94.2

[1] Calculated from measured values averaged for 1976 and 1977. Remainder of values calculated as a percentage of theoretical clear-sky insolation.

[2] Considered constant throughout the year.

available) were estimated by multiplying the theoretical clear-sky insolation by 0.78 (mean of $\overline{E}_m/\overline{E}_c$, Table 3) and then by 0.95 (1 - albedo of water). Table 4 also contains the estimated geothermal loading (considered constant throughout the year) between Stations A and B and a comparison of loadings from solar insolation and geothermal sources.

DISCUSSION

The geothermal power added to the Firehole River between Stations A and B was estimated as approximately 425 MW. This inflow, which is distributed along about 18.5 river kilometers accounts for an average temperature increase of 11 C of Station B over Station A. From Figure 21 it might appear that the bulk of the geothermal energy enters in the Upper Geyser Basin as the temperature increased 11 C from Station A to just below Iron Spring Creek while it increased only 4 C from Midway Geyser Basin to Station B and 4 C from Sentinel Creek to Nez Perce Creek. Actually less than half of the geothermal energy added between Stations A and B entered from the Upper Geyser Basin including Iron Spring Creek. Since the river discharge increases downstream, a given geothermal inflow results in a lesser temperature increase compared with the same inflow into a smaller upstream discharge. Furthermore, the higher excess temperature existing in the Middle and Lower Geyser Basins results in a greater temperature decay rate which tends to offset the temperature increases resulting from thermal inflows. The 4 C temperature increase from Sentinel Creek to Nez Perce Creek suggests that significant thermal additions occur in this reach. Only a few, small, geothermal features were observed visually or on the IR imagery (Fig. 18). These inflows by themselves were not of sufficient volume to account for the observed temperature increase. Sugmerged thermal springs, inflow from geothermally influenced groundwater, and solar insolation may have accounted for the differential.

The reasonably constant 425 MW entering the Firehole between Stations A and B would represent the waste heat discharged to a receiving water (of about 6-7 m^3/s discharge) by a 230 MW nuclear power plant (at 35% efficiency) or from a 425 MW fossil-fueled plant (at 40% efficiency with one-third the waste heat as stack loss). Coincidentally, in the latter, waste heat transferred to the receiving water equals net power production under these particular circumstances. These plants would be small by today's standards where 1,000 MW plants are common.

Solar insolation contributes a significant heat load to the river between Stations A and B ranging from an average 108 MW in July (25.4% of geothermal power input) to 26 MW in December (6.1% of geothermal). Although geothermal loading continues throughout the year as the dominant thermal factor, solar insolation is the greatest single factor in the diel fluctuations of stream temperature since geothermal inflows are essentially constant throughout the day. Values of 71-82% of possible clear-sky insolation in July and August resulted in an average 3-4 C fluctuation in water temperature. If 90-100% of clear-sky insolation were present the diel fluctuations could be increased an additional 1 C and the average temperature raised a corresponding amount.

A one-dimensional excess temperature computer model (Bauer and Mackenroth 1974) was applied to the two reaches used earlier in estimating dissipation of heat in the calculation of geothermal input (Results section). These reaches exhibited continuous temperature decay within the reach boundaries. The objectives were to determine if the observed decays could be explained by heat transfer to the atmosphere using reasonable values of wind speed, current speed, air temperature, and average depth. The temperatures obtained from the IR imagery of 21 October 1976, were used as input to the model.

The first reach investigated extended about 3.7 km from below Biscuit Basin to a point above Excelsior Geyser. The excess temperature at the beginning of the reach was taken as 11 C over an estimated natural temperature of 5 C (water temperature = 16 C, Figs. 15, 16, and 21). The observed decay in this reach was 1 C. The second reach was a 3 km section below Nez Perce Creek and had an excess temperature of 14 C over a natural temperature of 5 C (water temperature = 19 C, Figs. 19-21). The observed decay in this reach was 2 C.

Estimated wind speeds of 2.25-3.50 m/s, average depth of 0.5 m, air temperature of 4-8 C, current speed of 0.5 m/s, and a mass transfer coefficient of 2.68 x 10^{-8} (Jackman and Yotsukura 1977) were used. Calculated decay values were less than observed by about 0.1 degree/degree of decay. Manipulation of variables such as increase in wind speed or decrease in depth could have resulted in better agreement between calculated and observed values, however, conduction to the stream bottom (largely composed of bedrock) may have accounted for the remaining heat transfer (10% in these cases) not accounted for by transfer to the atmosphere. Loss of heat to bedrock accounted for 20-25% of the total heat transfer in studies by Brown (1969, 1972).

The Firehole River appears to have the ability to absorb a relatively large amount of "outside" heat and yet maintain viable populations of brown and rainbow trout in the warmest reaches. In evaluating this ability several factors which contribute to a low natural temperature (and consequently lower stream temperature after geothermal additions occur) must be considered.

Solar insolation has already been discussed with respect to its relationship to water temperature. Other factors which tend to suppress the natural temperature of the Firehole are moderately low relative humidity and consistent breezes (Wright and Horrall 1967), cool sources originating from snow melt and groundwater, moderately low daytime air temperature, cool nighttime air temperature, and relatively clear nighttime skies. Most of these factors also contribute to rapid decay of excess temperature through back radiation, evaporation, and conduction to the atmosphere. There is also the suggestion from the data that conduction to bedrock in the stream bottom may account for significant heat transfer. In the absence of any of these factors or with higher solar insolation or greater heat input from exogenous sources, higher water temperature would certainly result.

Kaya (1978b) determined an upper incipient lethal temperature of 26.2 C for juvenile Firehole rainbow trout acclimated at 21 or 24.5 C. In the Lower Geyser Basin summertime water temperature frequently exceeded this value. The highest mean monthly temperature recorded (26 C in July, 1977) was only slightly less than this upper incipient lethal temperature. The same study determined that for juvenile Firehole rainbow trout acclimated at 24.5 C, a 1 C increase in test temperature caused the time to 50% mortality to be reduced by a factor of 3.9. These findings would strongly suggest that any increase in maximum or mean temperature in the river in the Lower Geyser Basin would very likely have deleterious effects on the resident trout populations.

Although temperature values recorded at Station B were frequently well above the 26.2 C upper incipient lethal temperature determined by Kaya (1978b), no fish kills were observed during this study. Mortalities apparently associated with high temperature have been reported previously. Roeder (1961) cited temperatures above Nez Perce Creek in July, 1961, as high as 32.6 C and indicated the presence of an associated fish kill. An unusual event was reported by Park Ranger B. Riley McClelland (1960) in which he described hundreds of fish crowding into Iron Creek (Iron Spring Creek) and the Little Firehole River on 17 July 1960. About 150 dead fish were found near the

Firehole Cascades. The river temperature at this time at a point above Nez Perce Creek was measured at 28.3 C, a value lower than the 29.5 C maximum measured in the present study in which no fish kill was observed. In the absence of continuous recording, however, the highest temperature which preceded McClelland's observations is not known.

Sentinel Creek appeared to be an important cold-water refuge during July and August. Temperature of Sentinel Creek was about 10 C lower than that of the Firehole. Large numbers of brown and rainbow trout in all size classes were observed during these months of 1974-1977 in the lower several hundred meters of the stream. Over 500 trout were marked and released in Sentinel Creek in August of 1976 (Kaya et al. 1977). It was apparent that the trout were using Sentinel as a refuge only as no significant feeding activity was noted nor did this small stream appear capable of providing food organisms for the large numbers of fish observed. No spawning activity was observed nor did the time of observation correspond with the spawning periods of the trout species present.

Evidence indicated that most fish using Sentinel Creek originated downstream, however, some marked above Station B moved downstream in response to increasing summertime temperature and were eventually found in Sentinel Creek (Kaya 1978a). Obviously, not all fish were using Sentinel as it was quite far removed from reaches above Station B. Furthermore, sampling and visual observations during the months when fish were using Sentinel Creek revealed that fish were present in the high temperature of the main Firehole.

The thermal gradient associated with Sentinel Creek (Figs. 29 and 30) could certainly explain the attraction to Sentinel of any fish within this 1 km reach. The lower reaches of Nez Perce Creek might also be thought to be attractive as a cool-water refuge since it is cooler than the Firehole. Nez Perce is considerably warmer than Sentinel Creek, however, and its mouth is shallow and swift. No concentrations of fish were observed in Nez Perce Creek.

The distribution of trout in the Firehole River was described by Kaya (1978a). Above Kepler Cascades only brook and brown trout were found with brook trout accounting for 85% of the fish sampled. Just below Kepler Cascades, brown trout accounted for 98% of the fish observed, a distinct contrast with the populations above Kepler. Brown trout comprised 90% of the samples from above Midway Geyser Basin with rainbow trout accounting for the remainder. Below Midway Geyser Basin to the vicinity of Nez Perce Creek, rainbow trout accounted for 75% of the samples with brown trout making up the remainder, again a distinct contrast with the upstream reaches.

In the reach below Kepler Cascades a census estimated the brown trout population density in the range 1.8 ± 0.5 to 2.6 ± 1.2 fish/m ($P=.05$) during July-October, 1975. Large brown trout (>300 mm) migrated into this reach during late summer and fall of 1974 and 1975 ostensibly to spawn. It is not known where the large brown trout originated which moved into the area. No temperature barriers were detected with IR imagery above Midway Geyser Basin to prevent their originating from anywhere within this area.

In a reach above Station B the combined populations of brown and rainbow trout were estimated at 1.3 ± 0.5 fish/m in June, 1975, and 1.1 ± 0.6 fish/m (P=.05) in October, 1975. A census performed in August of the same year provided recapture rates too low to allow a reliable population estimate to be made. The poor success in recapture of fish in August suggested that fish were moving out of the census area. This movement was confirmed by recapture of fish marked within the census area from 300 m above to 2 km below the census area.

There was no evidence that fish moved upstream from the Lower Geyser Basin area to above Midway Geyser Basin. No fish marked below Midway were found above Midway. The species compositions of the two areas were in marked contrast with one another. The most prominent feature suspect in preventing upstream movement is Excelsior Geyser. Its discharge results in a pronounced gradient (Figs. 24-26) which very possibly inhibits upstream movement. The gradient expands nearly across the river about 200 m below Excelsior Geyser and may indeed repel upstream movement.

The thermal gradient pictured in Figures 27 and 28 occurred near the upper end of a study section chosen by Kaya (1977, 1978a).

Although the gradient extended across the width of the river at the time the imagery was made, some evidence exists that fish crossed this gradient in an upstream direction.

The reproductive biology of Firehole River trout was described by Kaya (1977). Brown trout below Kepler Cascades (above essentially all geothermal inflows) had normal gonadal development and reproduced well. Brown trout from below Midway Geyser Basin had poor reproductive success with a low percentage of gonads maturing among adults and prespawning degeneration of ova in females. Rainbow trout, present in significant numbers only below Midway, spawned in late fall and early winter in contrast to a normal spring spawning period. Redds were found within this area in December, 1975. Fertilized eggs were removed which later hatched into rainbow trout fry indicating rainbow trout stayed within the area to spawn.

The growth and diet of Firehole trout were described by Kaeding and Kaya (1978). Brown trout from below Midway Geyser Basin were longer at any given age than those from below Kepler Cascades. Scales from brown trout taken from below Midway indicated two growth periods per year instead of the more usual single period which was present below Kepler Cascades. The multiple growth periods resulted from early spring warming of the already elevated water temperatures below Midway Geyser Basin followed by cooling due to runoff followed in turn by a second warming trend as runoff subsided (Fig. 7). Growth of brown trout from below Midway appeared to be inhibited during the hot summer months as indicated by scale annulus formation. Rainbow trout from below Midway had growth patterns and length-at-age similar to brown trout from the same area. Trout from below Midway fed extensively on dipterans, molluscs, and ephemeropterans while trout from below Kepler Cascades fed heavily on trichopterans.

The maintenance of a viable trout population did not appear difficult in any reach of the Firehole River investigated except the section between Midway Geyser Basin and Nez Perce Creek. This reach may very well be marginal with respect to reproduction and survival of the brown and rainbow trout populations present. This is evidenced by previous accounts of fish kills, poor reproductive success of brown trout, apparent movement of fish out of the area during the summer months, inhibition of growth during summer, and the consistent use of Sentinel Creek as a cold-water refuge.

The argument could be made that downstream drift might sustain populations below Midway Geyser Basin. There is logic to this argument for brown trout which have breeding populations above Midway but not for rainbow trout for which breeding populations above Midway are very limited if, indeed, they exist at all. It is probable that the Firehole River below Midway Geyser Basin is consistently near the upper limits of temperature tolerance during the late summer months for the trout species present. It is very likely that this reach is capable of being pushed to and past those limits during periods of high ambient temperatures and/or low discharge (e.g. summer of 1977). Ironically, this reach appears to contain the best habitat with respect to stream morphology and perhaps this factor compensates to some extent for the stress induced by the high temperatures.

Any conclusions drawn from the Firehole River with respect to the capacity of streams, in general, to assimilate heat and yet maintain viable trout populations must be done with care. It must be remembered that the Firehole is in a high mountain setting with mild daytime temperature and cool nighttime temperature. Summertime solar insolation is approximately 20% less than the maximum possible. Relative humidity is fairly low allowing high dissipation of heat through high net negative longwave radiation, evaporation, and conduction. These factors undoubtedly contribute significantly to a temperature regime in the lower Firehole River in which trout can survive and reproduce. The incidence of the same thermal load on some other stream whose capacity for amelioration of high temperature is significantly less than that of the Firehole would very likely have more detrimental effects.

APPENDIX

Table 5. Station A temperature data (C).

Mo.	Days	Year	Avg. low	Avg. mean	Avg. high	Avg. range	Min.	Max.
July	18-31	1974	10.0	11.0	12.0	2.0	9.0	13.5
Aug.	22-31		8.5	10.5	13.0	4.5	7.5	13.0
Sept.	1-30		6.5	8.5	10.5	4.0	4.0	12.5
Dec.	1-19		1.5	2.0	2.5	1.0	0.0	4.5
April	1-30	1975	4.5	6.0	7.5	3.0	0.5	9.5
May	18-31		4.5	6.5	8.5	4.0	2.5	11.5
June	1-30		5.0	7.0	9.0	4.0	3.5	11.5
July	1-31		11.5	13.0	15.0	3.5	5.0	17.5
Aug.	1-25		10.0	12.0	14.0	4.0	7.0	15.5
Sept.	4-30		8.0	9.5	11.0	3.0	6.0	13.0
Oct.	13-31		5.0	5.5	6.0	1.0	2.0	8.0
Nov.	1-13		3.5	4.0	4.5	1.0	1.0	6.5
May	22-31	1976	5.0	7.0	9.0	4.0	4.5	11.5
June	1-30		6.0	8.0	9.5	3.5	5.0	13.5
July	1-31		11.0	12.5	14.5	3.5	9.0	16.5
Aug.	1-31		10.0	11.5	12.5	2.5	7.5	14.5
Sept.	1-30		9.0	10.0	11.0	2.0	6.5	13.5
Oct.	1-31		5.5	6.0	6.5	1.0	3.0	10.0
Nov.	1-30		3.5	4.0	4.0	0.5	0.0	7.0
Feb.	1-28	1977	2.0	2.5	3.0	1.0	0.5	5.0
April	5-30		4.0	6.5	9.0	5.0	2.5	11.0
May	13-31		6.5	8.0	9.5	3.0	5.5	15.5
June	1-30		11.0	13.5	16.0	5.0	8.5	20.0
July	1-31		11.5	14.5	17.0	5.5	9.5	19.0
Aug.	1-31		10.5	13.0	15.0	4.5	7.5	18.0
Sept.	1-11		8.5	11.5	14.0	5.5	7.0	15.5

Table 6. Station B temperature data (C).

Mo.	Days	Year	Avg. low	Avg. mean	Avg. high	Avg. range	Min.	Max.
Aug.	22-31	1974	19.0	21.0	23.0	4.0	18.0	24.0
Sept.	1-30		17.0	19.0	20.5	3.5	15.5	23.0
Nov.	1-30		14.0	14.5	15.0	1.0	12.0	16.5
Dec.	1-29		12.5	13.0	13.5	1.0	10.5	16.0
Jan.	3-31	1975	11.5	12.0	12.5	1.0	8.5	14.5
Feb.	17-28		13.0	14.0	14.5	1.5	11.5	15.5
Mar.	1-19		15.0	16.0	16.5	1.5	13.0	17.5
April	1-30		17.0	18.0	19.0	2.0	13.0	21.5
May	1-31		17.0	18.5	20.0	3.0	12.5	23.0
June	1-30		13.0	15.0	16.5	3.5	10.0	20.0
July	1-31		21.5	23.5	25.5	4.0	16.0	29.0
Aug.	1-31		21.5	23.0	25.0	3.5	18.0	27.0
Sept.	1-30		20.0	21.5	23.0	3.0	17.5	25.0
Oct.	13-31		15.5	16.0	16.5	1.0	13.5	21.0
Nov.	1-14		15.0	15.5	16.0	1.0	12.0	18.0
Dec.	20-31		13.5	14.0	14.5	1.0	12.5	15.0
Jan.	1-21	1976	13.0	13.5	14.0	1.0	11.0	17.5
Feb.	9-28		14.0	14.5	15.0	1.0	12.5	15.5
Mar.	1-11		14.5	15.5	16.0	1.5	12.5	18.5
May	23-31		11.0	12.5	14.0	3.0	10.0	16.0
June	1-30		15.5	16.5	17.5	2.5	12.0	23.5
July	1-31		22.5	23.5	25.5	3.0	20.0	28.0
Aug.	1-31		21.5	22.5	24.0	2.5	19.5	26.0
Sept.	1-30		20.5	21.0	22.0	1.5	18.0	24.5
Oct.	1-31		17.0	17.5	18.0	1.0	15.0	21.5
Nov.	1-30		15.0	15.5	15.5	0.5	11.0	18.5
Dec.	1-31		13.0	13.5	13.5	0.5	12.0	15.0
Feb.	1-28	1977	14.5	15.0	15.5	1.0	12.5	17.5
April	5-30		16.5	18.5	20.5	4.0	14.0	22.5
June	16-30		23.5	25.0	26.5	3.0	20.0	29.0
July	13-27		24.5	26.0	27.5	3.0	22.5	29.5
Aug.	11-31		23.0	24.5	26.0	3.0	18.5	29.5
Sept.	1-12		22.5	24.0	26.0	3.5	20.5	27.0

Table 7. Temperature data at noted locations on the Firehole River and its tributaries (C).

Mo.	Days	Year	Avg. low	Avg. mean	Avg. high	Avg. range	Min.	Max.
Above Midway								
May	18-31	1975	10.5	12.5	15.0	4.5	8.0	18.0
June	1-30		9.5	11.0	12.5	3.0	6.0	16.5
July	1-31		17.5	19.0	20.5	3.0	11.5	23.5
Aug.	1-31		17.0	18.0	19.5	2.5	14.0	21.5
Sept.	1-30		15.0	16.5	18.5	3.5	13.0	20.0
Sentinel Creek								
May	17-31	1975	3.0	7.0	11.0	8.0	0.5	17.0
June	1-30		8.0	10.5	13.0	5.0	4.0	18.5
July	1-31		13.5	16.0	18.5	5.0	11.0	21.0
Aug.	1-31		10.5	13.0	15.5	5.0	8.0	20.5
Little Firehole R.								
May	1-31	1976	5.0	7.0	9.0	4.0	1.5	13.5
July	1-31		15.5	17.5	19.5	4.0	13.0	21.5
Aug.	1-31		14.5	16.0	17.5	3.0	12.0	22.0
Sept.	1-30		12.5	13.5	14.0	1.5	10.0	16.5
Oct.	1-31		9.0	9.5	10.0	1.0	7.0	14.0
Nov.	1-30		7.5	8.0	8.5	1.0	2.5	11.0
Iron Spring Creek								
May	1-31	1976	14.5	16.0	18.0	3.5	12.0	20.5
June	1-30		15.5	17.0	18.5	3.0	14.0	22.5
July	1-31		19.5	20.5	22.0	2.5	18.0	23.5
Aug.	1-31		18.5	19.0	20.0	1.5	17.0	21.5
Sept.	1-30		17.0	17.5	18.0	1.0	16.0	20.0
Oct.	1-31		15.0	15.0	15.5	0.5	13.5	18.0
Nov.	1-12		15.0	15.0	15.5	0.5	14.0	15.5
Main Firehole above Iron Spring Cr.								
Feb.	1-28	1977	8.0	9.0	10.0	2.0	6.0	12.5
April	5-30		10.5	13.0	16.0	5.5	6.5	18.5
May	13-31		12.0	14.0	16.0	4.0	9.5	22.5
June	1-10		17.0	19.5	22.0	5.0	15.0	25.0

Table 8. Air temperature at Old Faithful Ranger Station (C).

Mo.	Days	Year	Avg. low	Avg. mean	Avg. high	Avg. range	Min.	Max.
Jan.	1-31	1975	-20.0	-12.5	-5.0	15.0	-38.5	3.0
Feb.	1-28		-17.0	-9.5	-2.0	15.0	-33.0	4.5
April	9-30		-9.5	-2.5	4.5	14.0	-18.5	8.5
May	1-31		-5.0	2.5	10.0	15.0	-15.5	19.5
June	1-23		-2.5	7.5	17.0	19.5	-1.0	26.0
July	1-31		4.5	15.5	26.5	22.0	-1.5	33.5
Aug.	1-31		2.5	12.0	21.5	19.0	-1.0	28.0
Sept.	1-19		-2.0	9.5	21.0	23.0	-2.0	35.0
Oct.	20-31		-6.5	-0.5	5.0	11.5	-15.5	10.5
Nov.	1-30		-15.0	-7.0	0.5	15.5	-29.0	16.0
Dec.	1-31		-13.0	-7.0	-1.0	12.0	-34.0	6.0
Jan.	1-31	1976	-16.5	-9.5	-2.0	14.5	-30.5	6.5
Feb.	1-29		-15.5	-8.0	-0.5	15.0	-38.0	5.0
Mar.	1-31		-17.0	-8.0	1.5	18.5	-33.5	11.0
April	1-30		-7.0	0.5	7.5	14.5	-18.5	15.5
May	1-31		-3.0	6.5	16.0	19.0	-10.0	19.5
June	1-30		-2.0	8.5	19.0	21.0	-6.5	28.5
July	1-31		3.0	15.0	27.0	24.0	-1.0	29.0
Aug.	1-31		0.0	11.0	22.0	22.0	-5.0	27.0
Sept.	1-30		-2.0	8.5	19.0	21.0	-9.5	27.0
Nov.	1-30		-10.0	-3.0	4.5	14.5	-34.5	13.0
Jan.	1-31	1977	-19.5	-11.5	-3.0	16.5	-33.5	7.0
Feb.	1-28		-18.0	-7.0	3.5	21.5	-29.0	13.0
Mar.	1-31		-16.0	-7.5	1.0	17.0	-29.5	11.0
April	1-30		-8.0	2.5	12.5	20.5	-24.0	22.0
May	1-31		-3.5	4.5	12.5	16.0	-13.0	20.0
June	1-30		-0.5	11.0	22.5	23.0	-5.5	28.5
July	1-31		2.5	14.0	25.5	23.0	-3.5	28.5
Aug.	1-31		2.0	13.0	23.5	21.5	-1.5	30.5
Sept.	3-14		-1.5	10.5	22.0	23.5	-6.5	25.5

Table 9. Total insolation from sun and sky on a horizontal surface at Old Faithful Ranger Station. (E = energy/d, kw-h/m^2; P = peak, clear-sky power, kw/m^2.) 1976.

	May		June		July		Aug.		Sept.		Oct.	
Day	E	P	E	P	E	P	E	P	E	P	E	P
1	...	...	7.6	...	8.6[1]	1.03	3.5	...	6.5	...	4.1	...
2	...	...	7.8	...	8.5	1.03	3.0	...	5.9	...	1.1	...
3	...	...	6.9	...	8.2[1]	1.01	4.1	...	6.4	0.89	2.7	...
4	...	...	8.6[1]	1.07	8.0	...	5.2	...	6.4[1]	0.87	2.5	...
5	...	...	8.4	...	8.0	...	6.7	...	6.0	...	1.7	...
6	...	...	5.4	...	8.0	...	7.8	...	2.6	...	2.8	...
7	...	...	7.3	...	7.5	1.01	7.9[1]	0.98	6.2	...	4.5	0.71
8	...	...	7.1	...	8.2	1.03	7.5	...	6.4[1]	0.90	4.4	0.71
9	...	...	8.2	...	9.0[1]	1.01	7.0	...	6.3[1]	0.87	4.3	0.70
10	...	...	7.6	...	8.7[1]	1.01	5.8	...	6.0	0.86	3.8	...
11	...	...	4.8	...	5.4	...	6.9	...	1.4	...	3.0	...
12	...	...	3.3	...	8.4	...	6.6	...	3.4	...	3.8	...
13	...	...	5.5	...	8.5	...	6.8	...	5.5	0.85	4.0	...
14	...	...	4.4	...	7.7	...	5.9	...	3.7	...	3.9	...
15	...	...	8.4	...	8.5	...	4.0	...	4.0	...	3.9	...
16	...	...	3.7	...	8.4	...	6.8	...	4.4	...	3.8	...
17	...	...	3.9	...	3.9	...	6.2	...	3.2	...	2.8	...
18	...	...	6.3	...	4.6	...	4.3	...	3.7	...	3.9	0.66
19	...	...	9.1[1]	1.14	7.0	...	7.3	...	2.7	...	3.8	0.66
20	...	...	7.4	...	5.3	...	7.0	0.94	4.0	...	3.7	0.63
21	...	...	6.0	...	7.4	...	7.2[1]	0.93	5.3	0.79	3.5	...
22	...	...	3.1	...	8.1	...	6.3	...	1.0	...	3.5	...
23	4.3	...	4.2	...	6.3	...	2.8	...	3.7	...	2.9	...
24	7.4	...	7.1	...	7.7	...	5.2	...	3.7	...	3.4	...
25	4.2	...	8.0	...	8.2[1]	0.98	6.3	...	3.1	...	0.8	...
26	8.1	1.08	9.2[1]	1.09	7.3	...	5.6	...	3.2	...	1.6	...
27	7.9[1]	1.07	8.9	1.07	5.7	...	6.9[1]	0.93	4.7	0.78	3.1	...
28	6.7	...	8.9[1]	1.07	7.7	...	6.8[1]	0.90	5.1[1]	0.77	3.2	0.57
29	8.5	...	7.0	...	5.5	...	6.8[1]	0.90	4.7[1]	0.74	1.9	...
30	8.5	...	7.5	...	4.7	...	5.2	...	4.8[1]	0.74	...	...
31	4.8	...	...	...	3.4	...	6.6	0.90	...	...	...	...
$\bar{x}$	6.7	...	6.7	...	7.2	...	6.0	...	4.5	...	3.2	...
Σ	60	...	201	...	222	...	186	...	134	...	92	...

[1] Entire day cloudless

Table 10. Total insolation from sun and sky on a horizontal surface at Old Faithful Ranger Station. (E = energy/d, kW-h/m^2; P = peak, clear-sky power, kW/m^2.) 1977.

	May		June		July		Aug.		Sept.	
Day	E	P	E	P	E	P	E	P	E	P
1	...	...	7.0	1.01	6.5	...	8.4[1]	0.97	6.8	...
2	...	...	7.5	...	4.0	...	6.6	...	6.7[1]	0.87
3	...	...	6.7	...	5.6	...	5.3	...	5.5	...
4	...	...	7.4	...	4.3	...	6.1	...	6.5[1]	0.87
5	...	...	8.7[1]	1.00	7.4	...	4.7	...	6.4[1]	0.85
6	...	...	4.2	...	8.5	...	5.4	...	5.9	...
7	...	...	5.3	...	8.8[1]	1.03	6.3	...	5.8	...
8	...	...	6.5	...	6.2	...	6.0	...	5.9	0.87
9	...	...	3.6	...	8.0	...	5.3	...	6.1[1]	0.86
10	...	...	3.1	...	5.5	...	6.4	...	6.0[1]	0.85
11	...	...	3.7	...	6.9	...	8.4[1]	0.96	5.5	...
12	...	...	7.8	...	8.4[1]	1.01	7.0	...	5.8[1]	0.84
13	...	...	6.8	...	7.3	...	6.7	...	5.8[1]	0.81
14	3.2	...	7.0	...	9.0[1]	1.03	6.2	...	5.1	...
15	4.6	...	8.0	...	8.9[1]	1.00	6.4	...	...	...
16	3.7	...	5.8	...	8.5	...	7.1	0.93	...	...
17	4.0	...	8.2	...	8.6[1]	0.98	6.4	...	...	...
18	2.2	...	5.5	...	8.3	0.98	2.9	...	...	...
19	2.7	...	6.5	...	8.5	...	5.9	0.93	...	...
20	6.0	...	4.9	...	6.5	...	5.0	...	...	...
21	7.6	...	4.3	...	4.5	...	5.3	...	...	...
22	4.5	...	8.6	...	6.5	...	5.0	...	...	...
23	4.3	...	8.5	...	5.1	...	7.0	...	...	...
24	4.1	...	7.7	...	1.4	...	4.2	...	...	...
25	3.8	...	9.0	1.01	7.8	...	3.8	...	...	...
26	4.0	...	7.4	...	6.5	...	1.9	...	...	...
27	5.2	...	7.8	...	7.3	...	4.4	...	...	...
28	6.7	...	8.9[1]	1.01	8.4	0.98	3.8	...	...	...
29	7.7	...	7.7	...	8.4[1]	0.98	3.0	...	...	...
30	7.5	1.05	8.9[1]	1.01	8.2[1]	0.98	3.3	...	...	...
31	8.6[1]	1.01	...	...	8.3[1]	0.98	4.9	...	...	...
$\bar{x}$	5.0	...	6.8	...	7.0	...	5.4	...	6.0	...
Σ	90	...	203	...	218	...	169	...	84	...

[1] Entire day cloudless.

REFERENCES CITED

REFERENCES CITED

Allen, E. T., and A. L. Day. 1935. Hot springs of Yellowstone National Park. Carnegie Institute of Washington. Publication 466. 525 pp.

Alt, D. D., and D. W. Hyndman. 1972. Roadside geology of the northern Rockies. Mountain Press Publishing Co., Missoula, Montana. 280 pp.

Argyle, R. L. 1966. Thermal dispersion in lotic waters of Yellowstone National Park. Master's thesis. Colorado State University, Fort Collins. 122 pp.

Bauer, D. P., and E. Mackenroth. 1974. One-dimensional stream excess temperature analysis. U.S. Geological Survey, Water Resources Div., Gulf Coast Hydroscience Center, Bay St. Louis, Mississippi. 31 pp.

Bennett, I. 1965. Monthly maps of mean daily insolation for the United States. Solar Energy 9(3):145-158.

Boettcher, A. J., R. M. Haralick, C. A. Paul, and N. Smothers. 1976. Use of thermal-infrared imagery in ground-water investigations, northwestern Montana. J. Res. U.S. Geol. Survey 4(6):727-732.

Bowen, I. S. 1926. The ratio of heat losses by conduction and by evaporation from any water surface. Physical Review 27:779-787.

Brown, G. W. 1969. Predicting temperatures of small streams. Water Resources Res. 5(1):68-75.

__________. 1972. An improved temperature prediction model for small streams. Water Resources Research Institute report WRRI-16, Oregon State Univ., Corvallis, Oregon. 20 pp.

Haines, A. L. 1977. The Yellowstone Story. Vol. I. Colorado Associated Univ. Press. 385 pp.

Hokanson, K. E. F., C. F. Kleiner, and T. W. Thorslund. 1977. Effect of constant temperatures and diel temperature fluctuations on specific growth and mortality rates and yield of juvenile rainbow trout, *Salmo gairdneri*. J. Fish. Res. Bd. Canada 34:639-648.

Jackman, A. P., and N. Yotsukura. 1977. Thermal loading of natural streams. Geological Survey Professional Paper 991. U.S. Govt. Print. Off., Washington, D.C. 39 pp.

Jobson, H. E. 1973. The dissipation of excess heat from water systems. J. Power Div., Proc. Am. Soc. Civil Eng. 99(PO1): 89-103.

Jones, R. D., J. D. Varley, R. E. Gresswell, D. E. Jennings, and S. M. Rubrecht. 1978. Fishery and aquatic management program; annual project technical report, Part I. U.S. Fish and Wildlife Service, Yellowstone National Park, Wyoming. 75 pp.

Kaeding, L. R., and C. M. Kaya. 1978. Growth and diets of trout from contrasting environments in a geothermally heated stream: The Firehole River of Yellowstone National Park. Trans. Am. Fish. Soc., 107(3):432-438.

Kaya, C. M., L. R. Kaeding, and D. E. Burkhalter. 1977. Use of a cold-water refuge by rainbow and brown trout in a geothermally heated stream. Prog. Fish-Cult. 39(1):37-39.

Kaya, C. M. 1977. Reproductive biology of rainbow and brown trout in a geothermally heated stream: The Firehole River of Yellowstone National Park. Trans. Am. Fish. Soc. 106(4):354-361.

__________. 1978a. Reproductive biology of trout in a thermally enriched environment: The Firehole River of Yellowstone National Park. Final Report prepared for the U.S. Dept. of Energy. Unpublished.

__________. 1978b. Thermal resistance of rainbow trout from a permanently heated stream, and of two hatchery strains. Prog. Fish-Cult. 40(4):138-142.

Krenkel, P. A., and F. L. Parker (Eds.). 1969. Biological aspects of thermal pollution. Vanderbilt Univ. Press. 407 pp.

Krenz, J. H. 1976. Energy conversion and utilization. Allyn and Bacon, Inc., Boston. 359 pp.

Macleod, I. D. G. 1970. Pictorial output with a line printer. IEEE Transactions on Computers C19(2):160-162.

McClelland, B. R. 1960. Temperature changes in the Firehole River-1960. Letter to Yellowstone National Park biologist W. R. Howe dated 10 Nov. 1960. Yellowstone National Park, Wyoming.

McKee, J. E., and H. W. Wolf (Eds.). 1963. Water quality criteria. California State Water Resources Control Board. 548 pp.

Morse, W. L. 1970. Stream temperature prediction model. Water Resources Res. 6(1):290-302.

National Academy of Sciences and National Academy of Engineering. 1972. Water quality criteria 1972. U.S. Govt. Print. Off., Washington, D.C. 594 pp.

Parker, F. L., and P. A. Krenkel. 1970. Physical and engineering aspects of thermal pollution. CRC Press, Cleveland, Ohio. 100 pp.

Raphael, J. M. 1962. Prediction of temperature in rivers and reservoirs. J. Power Div., Proc. Am. Soc. Civil Eng. 88(PO2): 157-181.

Roeder, T. S. 1961. Unpublished data.

Rosa, R. J. 1968. Magnetohydrodynamic energy conversion. McGraw-Hill, New York. 234 pp.

Selçuk, K., and J. I. Yellott. 1962. Measurement of direct, diffuse, and total solar radiation with silicon photovoltaic cells. Solar Energy 6(4):155-163.

Skinner, M. M., and J. E. Ruff. 1973. Applications of remote sensing to river mechanics. Vol. III. H. W. Shen, P. O. Box 606, Fort Collins, Colorado.

U.S. Bur. Reclamation. 1967. Water measurement manual. U.S. Govt. Print. Off., Washington, D.C. 327 pp.

U.S.G.S. (United States Geological Survey). 1974-1977. Water resources data for Montana. U.S. Dept. of Int., Washington, D.C.

Wilson, R. A., S. N. Hirsch, F. H. Madden, and B. J. Losensky. 1971. Airborne infrared forest fire detection system: final report. USDA Forest Service Research Paper INT-93. 99 pp.

Wright, J. C., and I. K. Mills. 1967. Productivity studies on the Madison River, Yellowstone National Park. Limnol. Oceanogr. 12(4):568-577.

__________, and R. M. Horrall. 1967. Heat budget studies on the Madison River, Yellowstone National Park. Limnol. Oceanogr. 12(4):578-583.